A STATEWIDE DEFLECTION STUDY

OF CONTINUOUSLY REINFORCED CONCRETE PAVEMENT IN TEXAS

by

B. F. McCullough
Supervising Design Research Engineer

and

Harvey J. Treybig
Engineering Assistant

Technical Report No. 46-5
for
Performance Study of Continuously
Reinforced Concrete Pavement
Research Project 1-8-63-46

The opinions, findings, and conclusions
expressed in this publication are those
of the authors and not necessarily those
of the Bureau of Public Roads.

ACKNOWLEDGMENTS

TABLE OF CONTENTS

LIST OF FIGURES

LIST OF FIGURES (Cont.)

LIST OF TABLES

ABSTRACT

This report is the climax to the performance study of continuously reinforced concrete pavement in terms of load-deflection studies. In this study the following factors affecting pavement performance were considered:

1. Subgrade support
2. Subbase type
3. Concrete modulus of elasticity
4. Concrete modulus of rupture
5. Pavement thickness
6. Season of the year
7. Soil moisture condition

The effect of each of the above factors on the deflection and stress or curvature is studied herein.

The variables that significantly affect deflection and radius of curvature are correlated into model equations. The constants in the equations were determined from the data using multiple regression techniques.

This report validates some initial assumptions made in the design and development of continuously reinforced concrete pavement for Texas conditions.

Report On

A STATEWIDE DEFLECTION STUDY
OF CONTINUOUSLY REINFORCED CONCRETE PAVEMENT IN TEXAS

I.   INTRODUCTION

Background

This report is a part of a continuing study by the
Texas Highway Department pertaining to the development
and design of Continuously Reinforced Concrete Pavement
(hereafter referred to as CRCP) in Texas. The Texas
Highway Department pioneered the use of CRCP in the
Southwest with the construction of an experimental pave-
ment in Fort Worth during 1951. Recent reports issued
by the Concrete Reinforcing Steel Institute indicate that
Texas now has more mileage of CRCP than any other state
in the Union.[1]

During the initial design development stages of CRCP
in Texas, several assumptions were made which the authors
wish to reiterate at this point. Among the initial
assumptions were the following:

1. To prevent pavement deterioration, the trans-
    verse cracks in the pavement must be of small
    enough magnitude to permit the retention of
    granular interlock and prevent the entrance
    of water. If sufficient granular interlock
    is maintained, then 100 per cent load trans-
    fer will be experienced across the crack and
    thus the pavement continuity will be maintained.[2]

2. The Westergaard Interior Loading Condition was
    used for determining the pavement thickness
    with additional steel being used at the edge
    to compensate for the difference in required
    thickness between an edge and interior loading
    condition. This approach results in a one to
    two inch thinner pavement than would be ob-
    tained with normal procedures used in designing
    jointed concrete pavements.[3, 4]

1

Although the AASHO Road Test provided valuable inform-
ation for use in the design and construction of rigid
pavements, numerous areas remain to be investigated
especially in the field of CRCP since this pavement type
was not covered at the Road Test.[5] The deflection
data obtained at the AASHO Road Test is difficult to
extrapolate to a formula for the design of continuous
pavement in Texas since: (1) it is not directly appli-
cable to this pavement type, (2) only one natural soil
type and strength was considered, (3) only one concrete
modulus of elasticity, and (4) lime stabilization was not
included.

In order to establish the effect of these parameters
and verify the original design assumptions, the Texas
Highway Department in 1963 initiated a large research
project to investigate the performance of continuously
reinforced concrete pavement. This is the fifth report in
connection with this study and the third relating to pave-
ment deflection. The earlier reports pertain to equipment
and technique development, deflection study on an experi-
mental pavement section, and a 24 hour deflection study on
several new untrafficked pavements.[6, 7, 8]

Since 1963, in excess of 15,000 individual measure-
ments of deflection, radius of curvature, crack width,
and temperature have been taken on numerous continuous
pavements located throughout the State. The schedule of
field observations is shown in Table 1.1. Many of the
procedures and techniques used are those developed at the
AASHO Road Test or modifications thereof.[5,6] Much
work has been done by the Texas Highway Department in
developing experimental techniques for studying CRCP.

Objectives of Study

The overall objective of this investigation is to
determine the effects of design variables on pavement
deflection and radius of curvature. After establishing
the parameters considered to be variables, a statistical
expression will be derived that can be used for calcu-
lating the deflection and radius of curvature produced

TABLE I.I

SCHEDULE OF FIELD OBSERVATIONS

RUN	SEASON	DATE RAN
I	FALL	OCT. — DEC. 1963
2	WINTER	JAN. — MAR. 1964
3	SUMMER	JUNE–JULY 1964
4	SPRING	MAR — APR. 1965

II.   DESCRIPTION OF EXPERIMENT

Factorial Design

The entire experiment was functional through a
factorial design that encompassed the variables involved
in pavement design. The chart which represents the
factorial experiment design is shown in Figure 2.1. In
order to represent each entry in the factorial design for
one pavement thickness, 90 different test sections would
be required. Figure 2.1 shows the entries in the fac-
torial table that were filled. Each symbol represents a
test section, therefore, a small degree of replication was
provided for. It was quite impossible to fully complete
the table due to the closely standardized design criteria.
In this report the test sections will sometimes be referred
to by number - (1-6) - which means Line one, Column six
on the factorial.

The variables which are represented in the factorial
are the controlled variables which are the subgrade
support, subbase type, concrete modulus of elasticity, and
concrete modulus of rupture. For pavement thickness simi-
lar charts were prepared. Figure 2.1A shows the jointed
pavement test sections in factorial arrangement.

Controlled Variables

In this experiment each level of the subgrade support
variable was grouped in accordance with the Texas Triaxial
Classification Chart.[9, 10] For this factorial, the
subgrades were classified as poor, fair, and good. Only
the strength parameter was used for classifying the sub-
grade support variable, with no attempt to further sub-
divide with index properties such as sand, clay, grading,
plasticity, etc. For each of these classifications, the
triaxial class range was as follows:[*]

-----

[*]In the Texas Triaxial Classification Chart, the numbers
 range from Class 1.0 to Class 6.0(+). The larger the
 number the weaker the material.

FIGURE 2.1

EXPERIMENT DESIGN FOR CONTINUOUSLY REINFORCED
CONCRETE PAVEMENT

X = 8" CRCP   Y = 6" CRCP

SUBGRADE SUPPORT	SUBBASE TYPE	SUBBASE MATERIAL	MODULUS OF ELASTICITY →	3,500,000 psi			5,500,000 psi			Line
			CONCRETE FLEXURAL STRENGTH →	Low 580 psi(−)	Medium 580-690 psi	High 690 psi(+)	Low 580 psi(−)	Medium 580-690 psi	High 690 psi(+)	
Poor 5.5 +	Non-Stabilized	Fine Grain			X Y			X X		1
		Crushed Stone			X X			X	X	2
	Stabilized	Cement			X	X		X X Y	X Y	3
		Asphalt			X Y	X		X		4
		Lime		X	X					5
Fair 5.0 – 5.5	Non-Stabilized	Fine Grain			X			X		6
		Crushed Stone			X	X				7
	Stabilized	Cement						X X		8
		Asphalt			X			X		9
		Lime			X					10
Good 4.0 – 5.0	Non-Stabilized	Fine Grain			X			X X X		11
		Crushed Stone			X			X	X	12
	Stabilized	Cement			X			X X X Y	X Y	13
		Asphalt			X					14
		Lime			X Y			X		15
Column →				1	2	3	4	5	6	

6

```
Poor:     Class     5.5     and       above

Fair:     Class     5.0     through   5.4

Good:     Class     4.0     through   4.9
```

The subbase was categorized into two general divisions, stabilized or unstabilized. Unstabilized subbases were subdivided into two basic categories - those with fine grain materials (natural sands) and granular material. The stabilized subbases were either lime, cement, or asphalt treated base material. As was the case with subgrade support, further subdivision in accordance with index properties was not considered. Therefore, a cement stabilized material may be an iron gravel, crushed limestone, a sand shell, etc. The subbases were generally constructed in accordance with the Standard Specifications of the Texas Highway Department.[11]

The modulus of elasticity* of the concrete pavement was based upon the type of coarse aggregate used. In Texas, experience indicates that concretes with siliceous river gravel coarse aggregate exhibit a modulus of elasticity of about 5.5 million psi, whereas, concretes with crushed limestone aggregate have a lower modulus of about 3.5 million psi. Thus it was on this basis of coarse aggregate source within the state that the modulus of elasticity of each pavement section was selected.

The modulus of rupture was divided into three categories. These three categories, low, medium and high represent concrete flexural strength ranges of less than 580, 580 to 690, and above 690 psi respectively.** Each of the modulus of elasticity levels was subdivided into these three levels of modulus of rupture. Most of the pavement sections entered in the factorial were in the medium range which is considered the optimum strength for CRCP.

---

*Tangent Modulus of Elasticity.

**Modulus of Rupture obtained with mid-point loading.

Pavement thickness, also a controlled variable could not be investigated to the extent desired because most of the CRCP in Texas is eight inches thick. There has been some six-inch CRCP built, but in a limited number of designs. Thus, it has been quite difficult to truly examine pavements with a lesser thickness than eight inches. Two different symbols are used in Figure 2.1 to represent the two pavement thicknesses considered.

Figure 2.1A shows the jointed pavement test sections. The three thicknesses are represented by symbols indicating the slab thickness. The sections represented in Column Two of Figure 2.1A are plain concrete and the sections in Column Five are reinforced. The load transfer at the trans-verse joints was by mechanical devices. This made it possible to make direct comparisons between jointed and continuous pavement. Everything was held constant in the factorial comparison except the pavement type.

Semi-Controlled Variables

Two other variables which were given due consideration but which are not shown on the factorial in Figure 2.1 are the season of the year and the general soil moisture condi-tion. The field data was taken in such a manner that all pavement test sections were studied in each of the four seasons of the year. The second semi-controlled variable was the general moisture condition of the soil. The general soil moisture condition is somewhat a function of the season. Data taken in winter and spring were in general, taken under wet conditions, the spring being more so. The data taken in summer and fall were taken under generally dry conditions.

Another parameter which was considered to be constant was the subbase thickness which was generally six inches plus or minus two inches. Studies at the AASHO Road Test found that subbase thickness has very little effect on pavement deflection in the range of 3 to 9 inches.[5] There-fore, the assumption of equal thickness is reasonable for the range of thickness considered, i.e. 4 to 8 inches. The cement factor for the concrete pavement is generally four and one-half sacks per cubic yard. The longidudinal reinforcement for the pavement was approximately 0.5 per cent in all cases.

FIGURE 2.1A

EXPERIMENT DESIGN FOR JOINTED CONCRETE PAVEMENT

J8 = 8" Slab J9 = 9" Slab J10 = 10" Slab

SUBGRADE SUPPORT	SUBBASE TYPE	SUBBASE MATERIAL	CONCRETE FLEXURAL STRENGTH	MODULUS OF ELASTICITY 3,500,000 psi			5,500,000 psi			Line
				Low 580 psi (−)	Medium 580-690 psi	High 690 psi (+)	Low 580 psi (−)	Medium 580-690 psi	High 690 psi (+)	
Poor 5.5 +	Non-Stabilized	Fine Grain			J10					1
		Crushed Stone			J9, J10			J8, J9, J10		2
	Stabilized	Cement								3
		Asphalt								4
		Lime			J9, J10					5
Fair 5.0 − 5.5	Non-Stabilized	Fine Grain						J8		6
		Crushed Stone			J10			J8, J9, J10		7
	Stabilized	Cement								8
		Asphalt								9
		Lime			J10					10
Good 4.0 − 5.0	Non-Stabilized	Fine Grain			J10			J9		11
		Crushed Stone			J9, J10			J8, J9		12
	Stabilized	Cement						J9, J10		13
		Asphalt								14
		Lime								15
Column				1	2	3	4	5	6	

6

Pavement Test Sections

The pavement sections which were used for test sections were essentially made up of three parts. These parts are the test section, transition area, and the replicate test section. The test section and the replicate test section are both 1200 feet long and separated by a 100 foot transition area as shown in Figure 2.2. Jointed concrete pavement test sections were layed out the same as the CRCP.

West of the Balcones Fault Zone through Central Texas, generally all pavements are flexible due to a combination of traffic density and availability of high grade flexible base construction materials. Consequently, the pavement test sections for this experiment were scattered throughout the eastern one-half of the State. Some of the criteria used in choosing the test sections were as follows:

1. The entire test section should be in a 2500 foot long tangent section with no grade in excess of one per cent.

2. Longitudinal reinforcement should be approximately 0.5 per cent steel.

3. The general soil conditions should be relatively constant as well as could be ascertained by engineering judgment and inspection.

4. The entire length, 2500 feet when in cut or fill sections, should be entirely therein to attain uniformity.

5. The structural components of the pavement must classify it into one of the 90 entries in the chart in Figure 2.1.

6. In no case were side hill sections chosen for test sections.

7. The subbase must extend the entire crown-width of the roadway. Trench type sections were not considered.

Table 2.1 gives a brief description of materials components, location, traffic applications, etc. of the pavement test sections studied in this experiment.
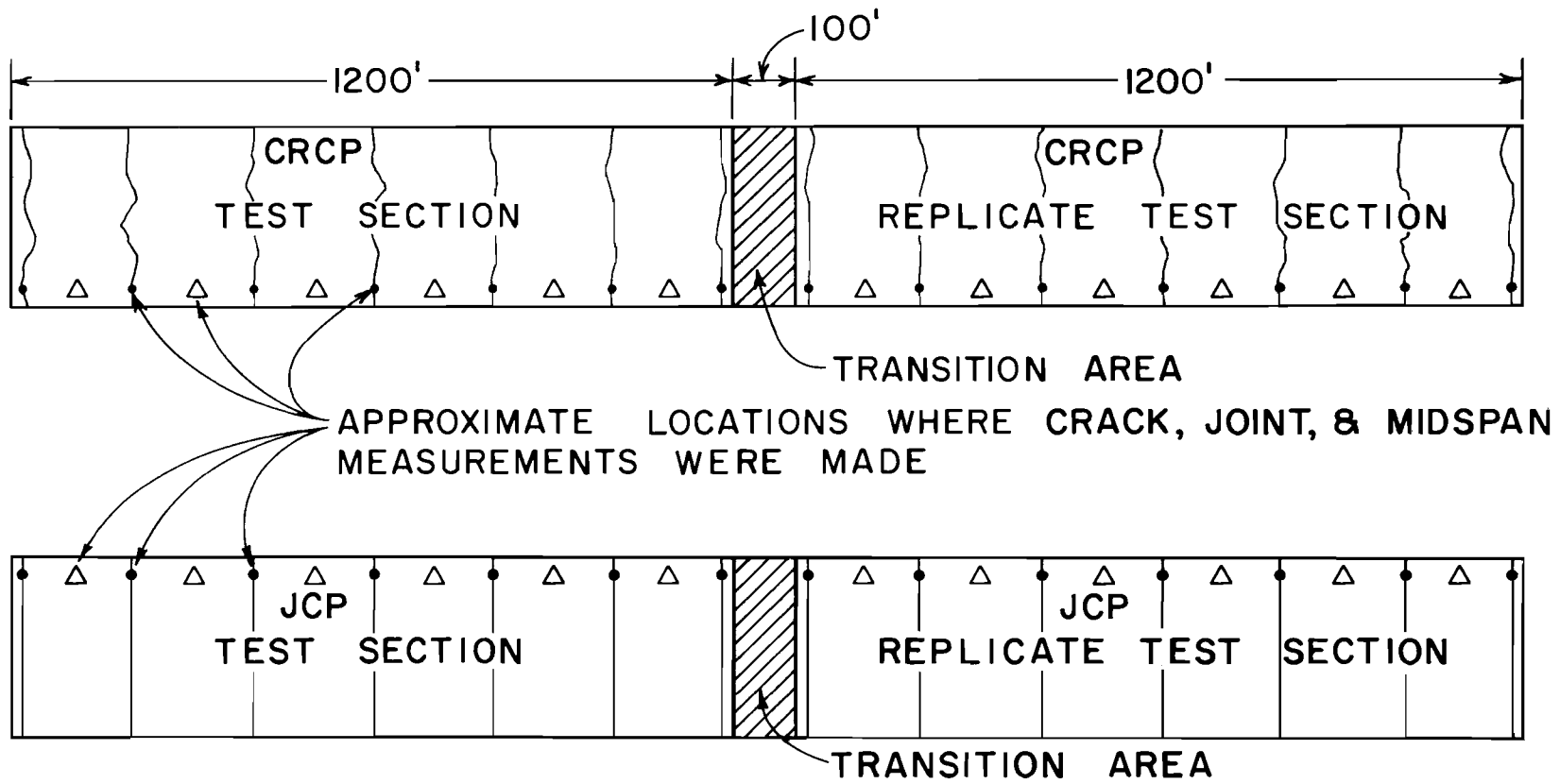
LAYOUT OF TEST PAVEMENTS

FIGURE 2.2

TABLE 2.1

DESCRIPTIVE INFORMATION RELATIVE TO SUBBASE AND SUBGRADE FOR THE TEST SECTIONS

Factorial Number Line-Column	Test Section Number	County	Highway	Subbase				Subgrade			Remarks (1)
				Type	Triaxial Class	Unconfined Comp. Stren.(2)	Stabilization	Type	Triaxial(3) Classification	Stabilization	
1-2	8-13-1	Tarrant	IH 820	Dark Brown Sand	1.0	117	6% Lime	Black Clay	5.5	5% Lime	6 in CRCP
1-2	8-13-2	Tarrant	IH 820	Dark Brown Sand	1.0	117	6% Lime	Shaley Clay	5.5	5% Lime	
1-5	675-7-1	Walker	IH 45	Crushed Sandstone	2.2	16.1	None	Sandy Clay	5.5 (1.0)	3% Lime	
1-5	675-7-2	Walker	IH 45	Crushed Sandstone	2.2	16.1	None	Sandy Clay	5.5 (1.0)	3% Lime	
2-2	95-4-1	Kaufman	IH 20	Crushed Limestone	1.0	50	None	Taylor Marl	5.5 (1.0)	4% Lime	
2-2	94-7-1	Dallas	SH 183	River Gravel	3.5	15.0	None	Del Borrow	5.5	None	
2-5	739-2-4	Jefferson	IH 10	6" Sand-Shell	2.0	65	None	Clay	6.0 (1.0)	4% Lime	
2-6	15-2-1	McLennan	IH 35	4" Bosque Gravel	3.4	20.9	None	Silty Clay	5.5 (1.0)	6% Lime	
3-2	739-2-7	Jefferson	IH 10	6" Sand-Shell	1.0	600	7.1% Cement	Clay	6.0 (1.0)	4% Lime	
3-3	156-7-1	Wichita	US 277	4" Sandstone	1.0	270	3.0% Cement	Clay	5.5	None	
3-5	739-2-2	Jefferson	IH 10	6" Sand-Shell	1.0	600	7.1% Cement	Clay	5.9 (1.0)	4% Lime	
3-5	500-3-3	Harris	IH 45	6" Sand-Shell	1.0	1100	7.0% Cement	Silty Clay	5.8	None	
3-6	27-13-1	Harris	US 59	6" Sand-Shell	1.0	1100	7.0% Cement	Silty Clay	5.6	None	
4-2	675-6-1	Walker	IH 45	4" Bituminous Concrete - (Crushed Sand-Stone)	1.0	226	5% OA-90 Asphalt	Sandy Clay	5.5 (1.0)	3% Lime	
4-3	156-7-2	Wichita	US 277	Sandstone	2.7	28	Asphalt	Clay	5.5	None	
4-5	495-10-1	Harrison	IH 20	6" Sandy Clay		30	Asphalt	Silty Clay	5.5	None	
5-1	14-16-2	Tarrant	IH 35	6" Clay	1.0	100	5% Lime	Clay	5.5	None	
5-2	8-13-3	Tarrant	IH 820	6"Lime Treated Subgrade	1.0	115	None	Dark Brown Clay	5.5	None	
6-2	14-16-1	Tarrant	IH 35W	Red Sand-Gravel	3.5	---	None	Black Clay	5.7	None	
6-5	495-4-2	Smith	IH 20	Natural Soil	4.0	6.5	None	Sandy Clay	5.0	None	
7-2	17-10-1	Bexar	IH 35	Crushed Limestone	1.0	41.0	None	Clay	5.5	3.5% Lime	
7-3	16-5-1	Comal	IH 35	Crushed Limestone	1.0	---	5% Lime	Clay	5.6	None	
8-5	500-3-2	Harris	IH 45	6" Sand-Shell	1.0	1100	7% Cement	Silty Clay	5.2	None	
8-5	739-2-1	Jefferson	IH 10	6" Sand-Shell	1.0	600	7.1% Cement	Clay	5.2 (1.0)	4% Lime	
9-2	675-6-2	Walker	IH 45	4" Bituminous Concrete	1.0	226	5% OA-90 Asphalt	Sandy Clay	5.2 (1.0)	3% Lime	
9-5	495-10-2	Harrison	IH 20	6" Sandy Clay		30	Asphalt	Sandy Clay	4.5	None	
10-2	442-2-1	Dallas	US 67	River Gravel	2.0	15.0	3% Lime	Del Borrow	5.2	None	
11-2	495-4-3	Smith	IH 20	Foundation Course	3.5	16.9	None	Sandy Clay	4.0	None	
11-5	495-4-1	Smith	IH 20	Foundation Course	4.0	6.5	None	Sandy Clay	4.0	None	
11-5	675-7-3	Walker	IH 45	Crushed Stone	2.2	16.1	None	Sandy Clay	4.6 (1.0)	3% Lime	
12-2	9-11-1	Dallas	IH 20	River Gravel	3.5	15	None		4.0	None	
12-5	739-2-5	Jefferson	IH 10	6" Sand-Shell	2.0	65	None	Clay	4.5 (1.0)	4% Lime	
12-6	15-2-2	McLennan	IH 35	Austin Chalk	3.4	20.9	None	Silty Clay	4.5 (1.0)	6% Lime	
13-2	739-2-6	Jefferson	IH 10	6" Sand-Shell	1.0	600	7.1% Cement	Clay	4.5 (1.0)	4% Lime	
13-5	271-14-3	Harris	IH 610	6" Sand-Shell	1.0	1100	7.0% Cement	Sandy Clay	4.8	None	
13-5	535-8-1	Colorado	IH 10	Sand	1.0	492	4% Cement	Silty Clay	4.6	None	
13-5	610-7-2	Bowie	IH 30	8" Sandy Clay	1.0	315	Cement	Sandy Clay	4.5	None	
13-6	271-14-1	Harris	IH 610	6" Sand-Shell	1.0	1100	7.0% Cement	Sandy Clay	4.8	None	
14-2	675-6-3	Walker	IH 45	4" Bit. Conc.	1.0	226	5% OA-90 Asphalt	Sandy Clay	4.5 (1.0)	3% Lime	
15-2	8-13-4	Tarrant	IH 820	Shaley Clay	1.0	100	5% Lime	Shaley Clay	4.5	None	
15-5	610-7-1	Bowie	IH 30	6" Clay Gravel	1.0	175	Lime	Sandy Clay	4.5	None	
12-2	9-11-2	Dallas	IH 20	River Gravel	1.0	114	3% Lime		4.0	None	
15-2	581-1-1	Dallas	Loop 12	River Gravel	1.0	70	3% Lime	Houston Clay	4.5 (1.0)	4% Lime	6 in CRCP
2-2	14-16-3	Tarrant	IH 35N	6" Flex. Base	3.5	---	None	Clay, rocky	5.5	Mechanical	
2-2	1068-1-1	Tarrant	TH 20	6" Flexible Base	3.0	---	None	Clay, rocky	5.5	Mechanical	
11-5	675-7-4	Walker	IH 45	Crushed Sandstone	2.2	16.1	None	Sandy Clay	4.6 (1.0)	3% Lime	

NOTE: (1) Unless specified otherwise in the "Remarks" Column all pavements are 8" CRCP.

(2) Unconfined compressive strength at an age of seven days tested in accordance with THD procedures.

(3) Classifications in parenthesis are after addition of lime to subgrade material.

III. METHOD OF ANALYSIS AND ACCURACY

The voluminous amount of data taken in this experiment required a careful and detailed analysis to obtain the desired end product. The 1604-A Control Data Computer was used to facilitate the analysis of the data to the extent that the computer could be used.

The computer program for the data reduction was written in such a fashion that all the pertinent data gathered would be presented for analysis. All data taken in the field were recorded on a data sheet, a copy of which is exhibited in Appendix B. The data was key-punched from this data sheet, then processed, stored permanently on magnetic tape, and printed out. The print-out included the following: the pavement depth, identification of the test section, average crack spacing, general moisture condition of the soil, deflection data, crack width data, radius of curvature data, temperature data, and a statistical analysis of the temperature, deflection, radius of curvature, and crack width data. Also included on the computer print-out were the average deflections corrected to a zero degree temperature differential.[6] A typical print-out is shown in Appendix C.

It should be emphasized here that each data point used in the following discussions and analysis represents the average of numerous readings. For each type of data point, the magnitude used to represent a test section was derived from an average of at least 14 data points.

Method of Analysis

The data was analyzed by investigating one variable at a time, i.e. holding all others constant. By using this method, it was possible to determine if the variable being studied was truly a variable or not. This method of having all but one variable constant in a comparison was made possible by the factorial design shown in Figure 2.1 For example, in comparing subgrade support any factorial entry under "Poor" could be compared with a corresponding entry under "Fair" or "Good". This

comparison would be clean, i.e. the subgrade support being the only variable. This same procedure was used to investigate each variable under consideration in this study. Analysis of variance techniques were used on several of the parameters, however, not enough entries were filled in the factorial to validate the analysis of variance results, even though some trends were shown.

Accuracy of Data

In order to qualify the data, it was necessaay to compare the accuracy of the measurements by type and position within each test section. The likeness of the data taken from pavement sections of identical design located throughout the State of Texas indicates quality data and good experimental technique. The following analysis was made to obtain a measure of the accuracy within a test section and a measure of the accuracy between replicate test sections in the same factorial entry.

Replication Within Test Section.
For each individual test section, the standard error of the mean was calculated for deflection and radius of curvature measurements taken at both the crack and midspan positions. The average of these respective measurements was then calculated for each of the four individual runs; the results of which are shown in Table 3.1. The error within a section presented here is well within the measuring accuracy of the equipment used. The deflection replication within a section is less than 0.001 inch in all cases, this magnitude is considerably less than the resolution of the Benkelman Beam ($\pm$0.002 inch).[12] The standard errors for the radius of curvature measurements are somewhat larger than the resulution (80 feet) or replication error (250 feet) of the Basin Beam.[6]

Replication Between Test Sections.
To determine the error between equivalent test sections, the standard error of the mean for the test sections within a given factorial block was determined. Only factorial blocks that had replicate sections were used in this analysis, and the number of replicate sections varied from one to two. It should be pointed out that these replicate

TABLE 3.1

STANDARD ERROR OF THE MEAN
DEFLECTION AND RADIUS OF CURVATURE

DATA RUN NUMBER	DEFLECTION		RADIUS OF CURVATURE	
	Crack	Midspan	Crack	Midspan
1	0.000904	0.000911	541	1193
2	0.000818	0.000766	586	935
3	0.000785	0.000781	583	861
4	0.000647	0.000675	1013	1172

sections were sometimes in different geographical area of the state such as Houston and Tyler. After determining the standard error of the mean for each of the applicable factorial blocks these values were then averaged for the four data runs. The standard errors found were as follows:

Deflection:

Crack Position = ± 0.00172 inch

Midspan Position = ± 0.00127 inch

Radius of Curvature:

Crack Position = ± 1525 feet

Midspan Position = ± 2079 feet

The above results indicate that the error for the data in any factorial block did not significantly exceed the measuring capability of the equipment used. Furthermore, the small error lends credence to assumptions that the test sections were properly classified in the factorial design for this experiment.

IV. ANALYSIS OF DATA

In this chapter, the data analysis will be presented in such a manner that one variable is studied at a time. The radius of curvature data was converted to stress by simple calculation and analyzed in terms of stress rather than the field measurement of radius of curvature. This method of conversion was covered in a previous report on this project.[6] The data is presented in bar graph fashion where it is weighted relative to the total for any type of measurement so that the sum of the four runs is equal to 100 per cent. The data from all four runs are summarized in factorial form in Appendix B.

Controlled Variables

The controlled variables, as previously defined, are the first to be considered in this analysis. The controlled variables are broken into the categories of support properties, concrete properties and slab thickness and type.

Support Properties. The strength property of the subgrade and its effect on deflection and stress at the crack and midspan position is investigated by comparing data from test sections which were identical except for the subgrade. These comparable sections were taken from the factorial. The weaker subgrade was evaluated in comparison with the better subgrade. There are three basic comparisons for each of the identical sections (except for subbase) i.e., poor to fair, poor to good, and fair to good. The comparisons were made by season or data run and by the total for the four seasons.

Figure 4.1 shows how the subgrade affected deflection in terms of the per cent of the comparisons made. In each of the four seasons the pavements on the weaker subgrade deflected more than comparable pavements on better subgrades. Considered: (a) total comparison, (b) weaker subgrade deflection more than the better subgrade in 67 per cent of the comparisons.
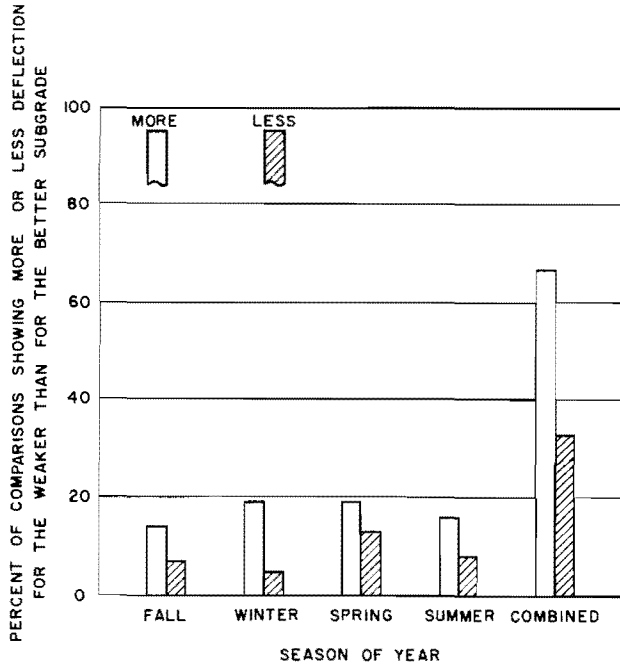
DEFLECTION COMPARISON OF A WEAKER
SUBGRADE WITH A BETTER SUBGRADE

FIGURE 4.1
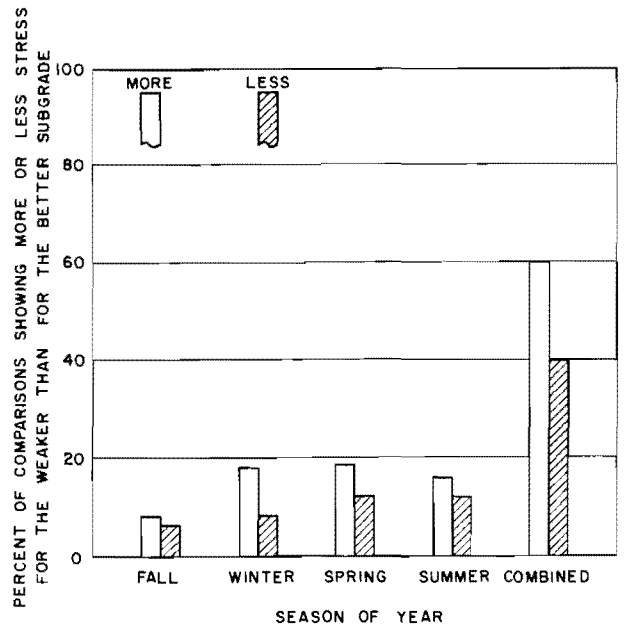
STRESS COMPARISON OF A WEAKER
SUBGRADE WITH A BETTER SUBGRADE

FIGURE 4.2

DEFLECTION COMPARISON OF EACH SUBBASE
WITH THE OTHER FOUR TYPES

FIGURE 4.3

STRESS COMPARISON OF EACH SUBBASE
WITH THE OTHER FOUR TYPES

FIGURE 4.4

Figure 4.2 shows how the subgrade affected concrete pavement stress in terms of the per cent of comparisons made. As was the case with deflection, the pavement with the weaker subgrade experienced more stress than one with a better subgrade 60 per cent of the time. In all four seasons the pavement with the weak subgrade generally had more stress than one with a better subgrade.
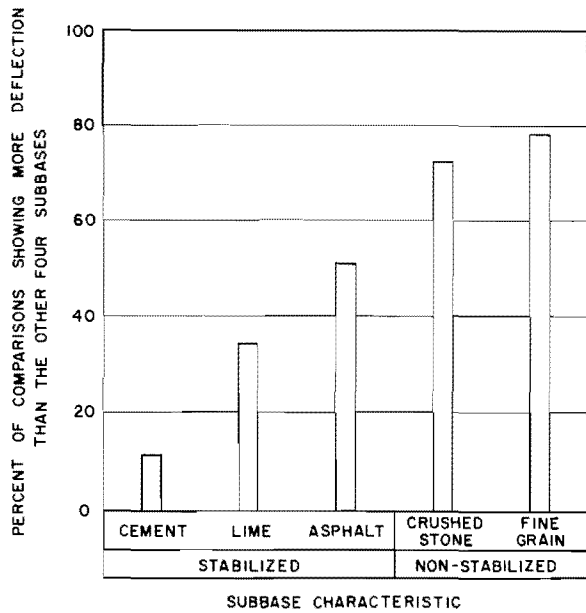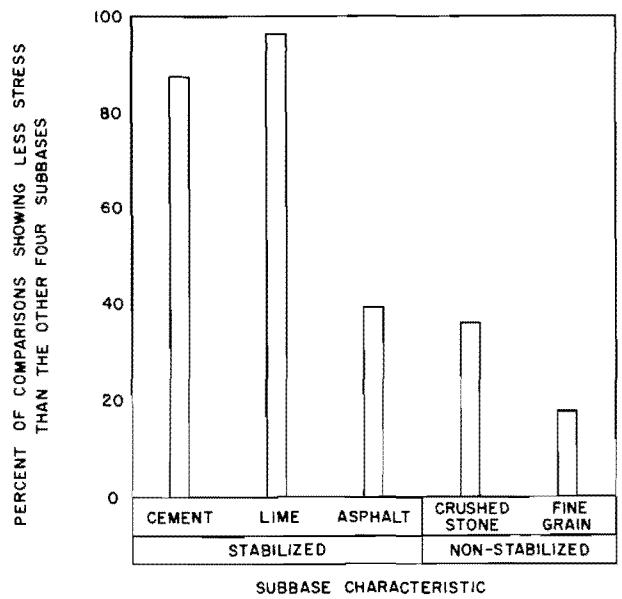
Inspection of Figures 4.1 and 4.2 indicates that deflection and stress are directly related to the subgrade support quality, i.e., the better the subgrade, the less deflection and stress there will be. The results for each season indicate this trend. It has been shown that CRCP with poor subgrade deflected 19 and 25 per cent more on the average than CRCP with fair and good subgrade respectively. Also pavement with a fair subgrade deflected nine per cent more on the average than did the pavement with the good subgrade.

Calculations show that the CRCP with the poor subgrade had approximately the same stress as did the one with the fair subgrade; however, the pavements with the good subgrade had 15 per cent less stress than the CRCP with the poor subgrade.

The subbases that were included in this study were evaluated on a comparative basis with all other variables constant. The deflection of a test section was compared with the deflection on all other types of subbases on the same subgrade class. The results for each subbase type were evaluated for each of the four seasonal data runs. The results for each season followed the same general trend. Figure 4.3 compares the subbases in terms of deflection on a percentage of comparisons basis (compilation of all four runs). The stabilized subbases appear to be superior to the non-stabilized materials as far as deflection is concerned. The stress analysis showed in general the same trends with respect to the subbase characteristic. These trends are shown graphically in Figure 4.4.

Concrete Properties. The two properties of the concrete which are part of this analysis are the modulus

of elasticity and the modulus of rupture or flexural
strength. The modulus of elasticity was determined from
the type of coarse aggregate in the concrete. Concrete
with siliceous river gravel is referred to as high modulus
and that with crushed stone is referred to as low modulus
of elasticity concrete. In Figure 4.5 for each data run
and all runs combined the deflection is compared on the
low and high modulus concrete. On the ordinate the per
cent of comparisons is plotted in which the low modulus
of elasticity concrete deflected more or less than the
high modulus of elasticity concrete. For each season
except fall the graph has two entries. The cross hatched
bar shows the per cent of comparisons made in which the
low modulus of elasticity concrete deflected less than
the high and the plain bar indicates the comparisons in
which low modulus deflected more than the high modulus
of elasticity concrete. The range of modulus of elasticity
experiencing the most deflection apparently varies slightly
with season. Calculations have shown that on the average,
the lower modulus of elasticity concrete in general
deflected 7.4 per cent less than the high modulus of
elasticity concrete. This finding, although contrary
to rational reasoning, is in line with that found in
another experiment.[7]

Figure 4.6 is bar graph comparing modulus of elas-
ticity against stress in the concrete slab. The graph
structurally is the same as in Figure 4.5 except that
this one graphically portrays stress in the concrete.
Inspection of Figure 4.6 shows that more comparisons of
stress on low and high modulus of elasticity concrete
showed less stress in the low than the high modulus
concrete. The range of modulus of elasticity experiencing
the most stress, also varies with season.

The second concrete property considered here is the
modulus of rupture. The analysis of the modulus of
rupture was made by determining whether the deflections
and stresses were more or less for the lower modulus of
rupture concrete than the higher modulus of rupture CRCP.
The evaluation was made for each season and also the
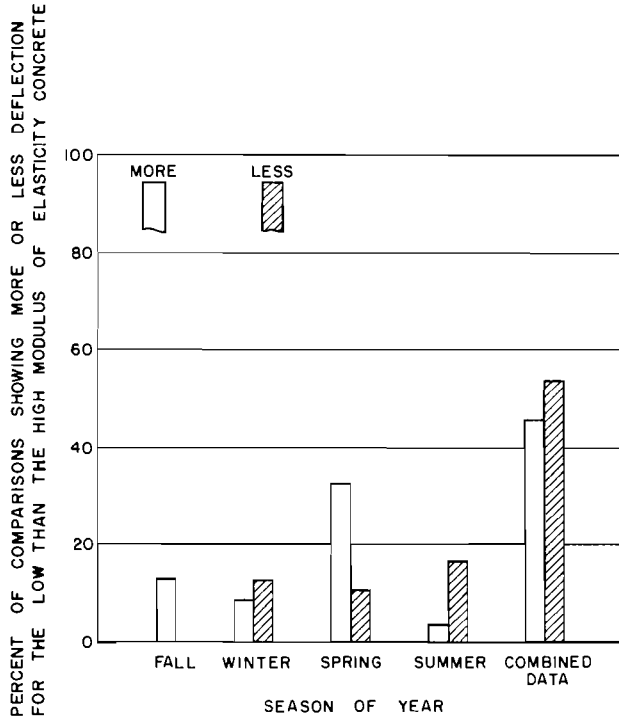
DEFLECTION COMPARISON OF LOW AND HIGH MODULUS OF ELASTICITY CRCP

FIGURE 4.5
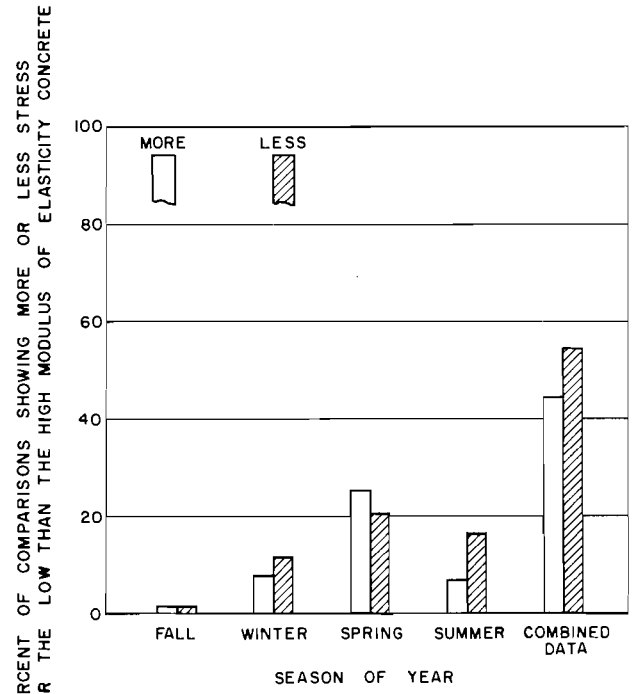
STRESS COMPARISON OF LOW AND HIGH MODULUS OF ELASTICITY CRCP

FIGURE 4.6
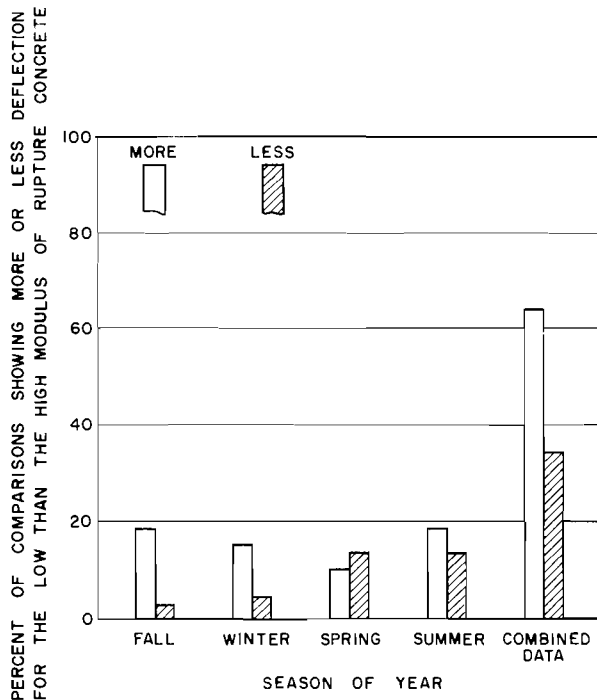
DEFLECTION COMPARISON OF LOW AND HIGH MODULUS OF RUPTURE CONCRETE

FIGURE 4.7
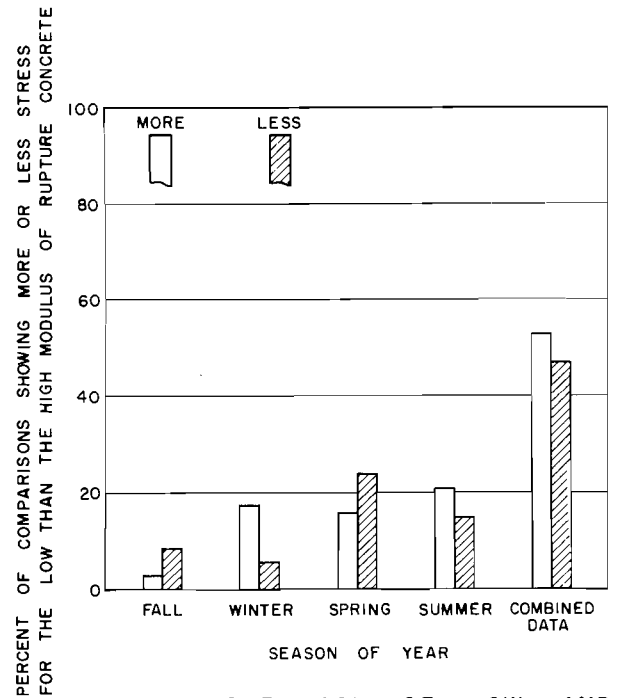
STRESS COMPARISON OF LOW AND HIGH MODULUS OF RUPTURE CONCRETE

FIGURE 4.8

combined data. Figure 4.7 portrays in bar graph style
the percentage of comparisons in which deflections on
the high modulus of rupture concrete were more or less than
those on the low modulus of rupture concrete. Note that
the low modulus of rupture concrete deflects more than
does the high. This was true for all seasons except for
the spring. The combined data also show that the average
deflection for all seasons is greater on the low modulus
of rupture concrete.

The comparison of stresses on the low and high modulus
of elasticity concrete indicate that on the average,
stresses were higher in the low than the high modulus of
rupture concrete. Figure 4.8 shows the per cent of
comparisons in which the stress was higher or lower than
that in the low modulus of rupture concrete.

Slab Thickness and Type. The pavement slab thick-
ness analysis was made by comparing deflection measure-
ments from sections that had identical classifications in the
factorial, but different slab thickness. This enables a
clean comparison of thickness to deflection and stress.

In each case the smaller thickness of concrete pave-
ment was compared with a greater thickness. The results
were combined for all four data runs. The comparison may
not be real good because of the small number of sections
compared.

Table 4.1 is a summary of the results obtained in
comparing pavements of different thickness and type. In
comparing six inch CRCP with eight inch CRCP, it was found
that the six inch pavement deflected 41 per cent more at the
crack position than did the eight inch CRCP. Comparing
eight inch CRCP with nine inch JCP, it was found that the
CRCP deflected on an average of 13.1 per cent less than
the JCP. When the eight inch CRCP was compared to ten
inch JCP, it was found that the CRCP deflected on an
average of 38 per cent less than the ten inch JCP.

It has been assumed in the past that 10 inch jointed
concrete pavement performance would be very much the same
as that of eight inch continuously reinforced concrete

TABLE 4.1

PERFORMANCE OF RIGID PAVEMENT IN TERMS OF THICKNESS, PAVEMENT TYPE, AND LOAD POSITION *

PARAMETER INVESTIGATED / LOAD POSITION / THICKNESS COMPARISON CRCP vs. CRCP / THICKNESS COMPARISON CRCP vs. JCP		DEFLECTION		STRESS	
		CRACK OR JOINT	MIDSPAN	CRACK OR JOINT	MIDSPAN
6" vs 8"		41.1	54.6	11.0	1.1
8" vs 9"		−13.1	30.8	−50.2	−11.1
8" vs 10"		−38.0	−28.5	−49.6	6.9

* NUMBERS IN TABLE INDICATE THE AVERAGE PERCENT DIFFERENCE FOR THE RESPECTIVE CONDITION

pavement.[4] Performance measured in terms of deflection shows that the eight inch continuously reinforced pavement is superior to the 10 inch jointed pavement. In Figure 4.9 deflections as computed by the equations developed herein are plotted against deflections measured on comparable 10 inch jointed concrete pavement. The deflections for both pavement types have been corrected to zero temperature differential, and the deflections for CRCP were corrected to an eight foot crack spacing and a 0.014 inch crack width. The data shows a remarkable relation between the two parameters. By forcing the correlation line through zero (a rational approach), the slope of the line indicates a ten inch JCP deflects 1.6 times more than an eight inch CRCP.

Deflection Position. On each test section a midspan deflection (between cracks) was obtained each time a reading was taken at the crack position. Figures 4.10 to 4.13 are plots of the average crack deflection versus the midspan deflection for each of the four runs. Although there is an off-set on the vertical axis (crack deflection) greater than zero, it may be stated that the edge deflection and crack deflection are approximately equal on any range of support properties with continuous pavements that have 0.5 per cent longitudinal steel or greater.

The radius of curvature measurements were also plotted in the same manner as deflection measurements and these results are illustrated in Figures 4.14 through 4.17. In the case of radius of curvature – in contrast to deflection – the crack position has considerably less magnitude than the midspan position, which means that the concrete at the crack position is experiencing considerably more stress.

In terms of deflection and radius of curvature, it is evident that the aggregate interlock produces adequate load transfer across a crack, but the transverse cracks affect the continuity condition of the slab.

Semi-Controlled Variables

Two factors which were studied on semi-controlled basis were the season of the year the field measurements
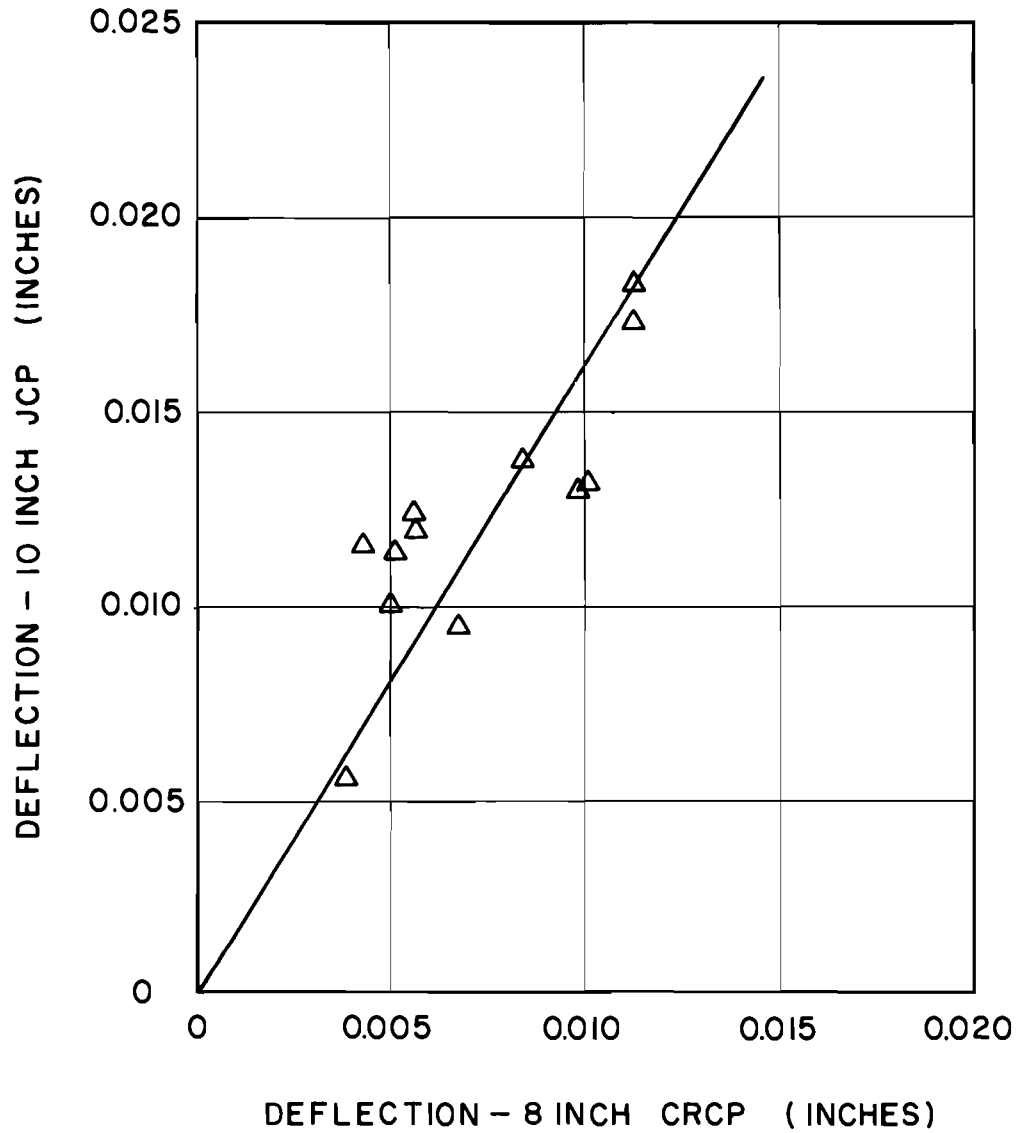
CALCULATED EIGHT INCH CRCP
DEFLECTION VS. MEASURED TEN
INCH JCP DEFLECTION

FIGURE 4.9

Dc =0.888 De + 0.0024
r² = 0.573
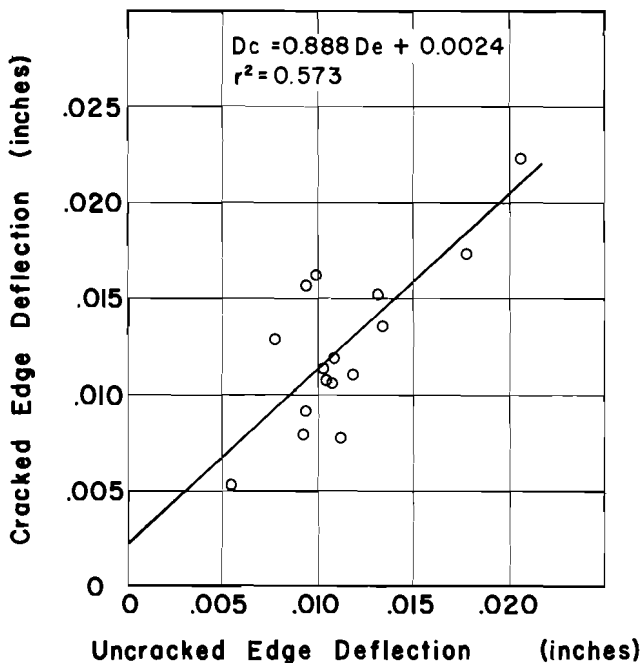
CRACKED EDGE vs. UNCRACKED EDGE
DEFLECTION — FALL

Figure 4.10

Dc = 1.088 De + 0.0007
r²= 0.623
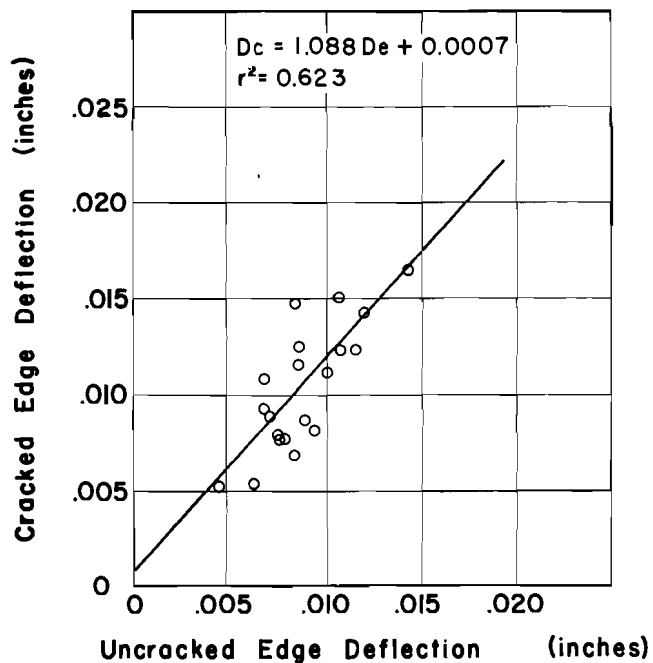
CRACKED EDGE vs. UNCRACKED EDGE
DEFLECTION — WINTER

Figure 4.11

Dc = 0.890 De + 0.0010
r²=.859
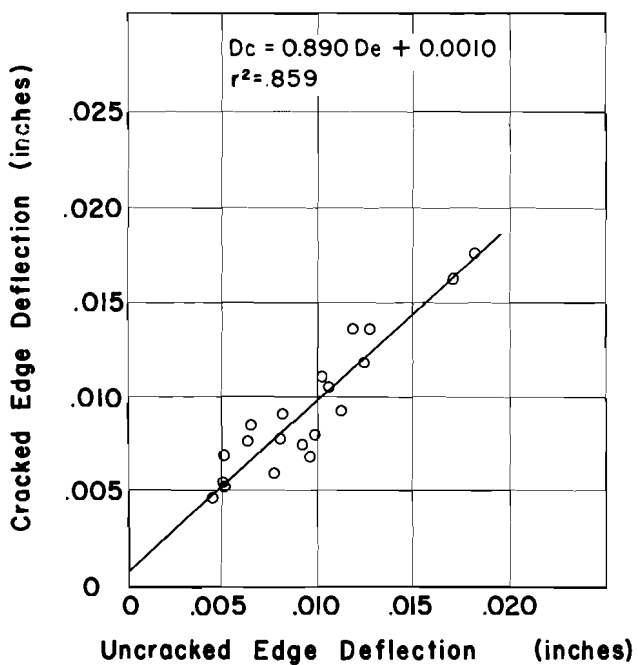
CRACKED EDGE vs. UNCRACKED EDGE
DEFLECTION—SUMMER

Figure 4.12

Dc = 0.913 De + 0.0014
r = .868
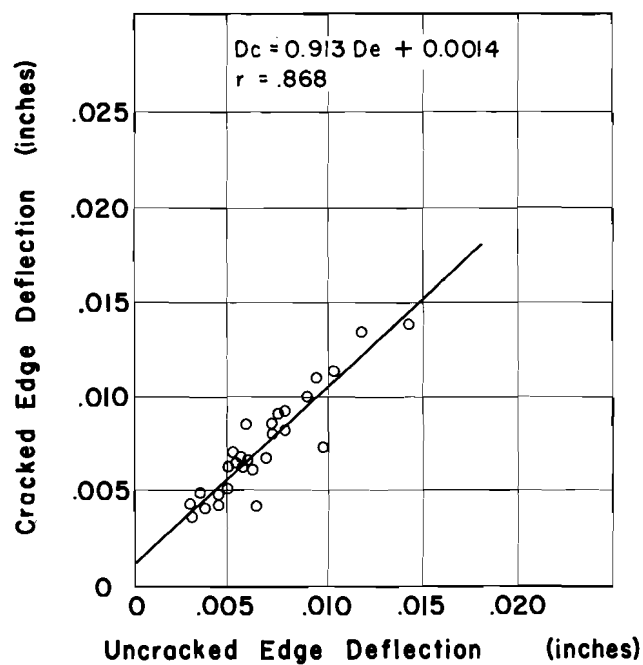
CRACKED EDGE vs. UNCRACKED EDGE
DEFLECTION — SPRING

Figure 4.13
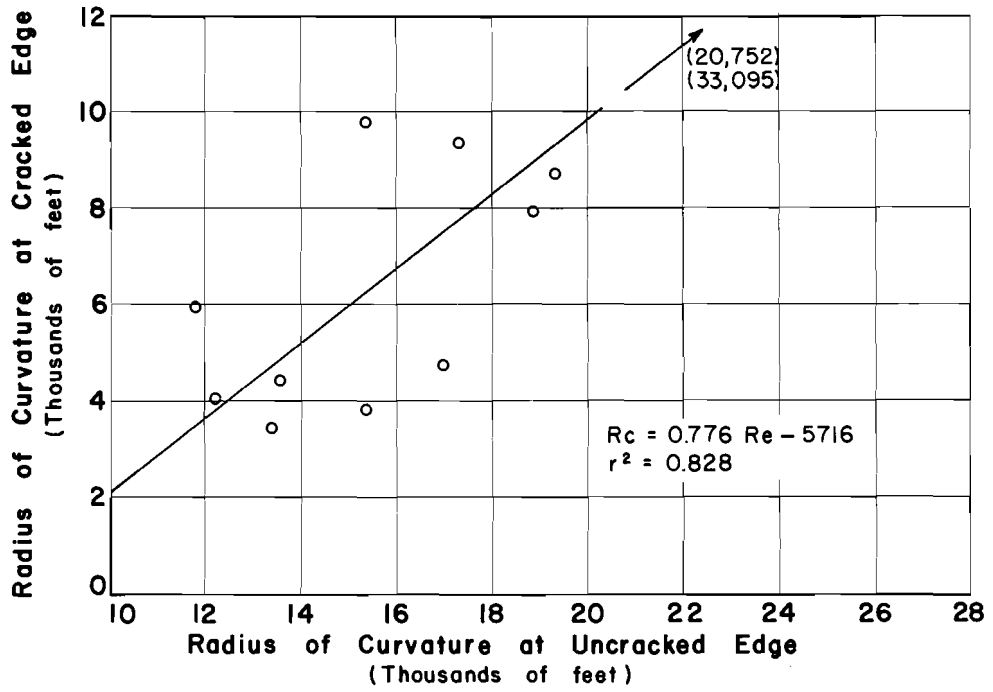
CRACKED EDGE VS. UNCRACKED
EDGE RADIUS OF CURVATURE

FALL

Figure 4.14
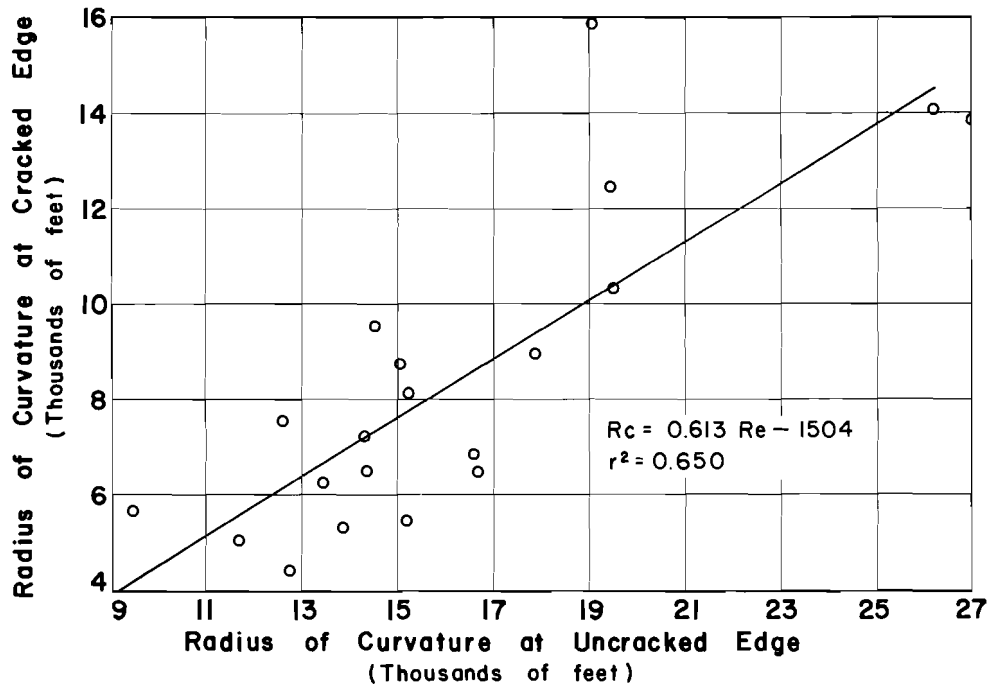
CRACKED EDGE VS. UNCRACKED
EDGE RADIUS OF CURVATURE

WINTER

Figure 4.15
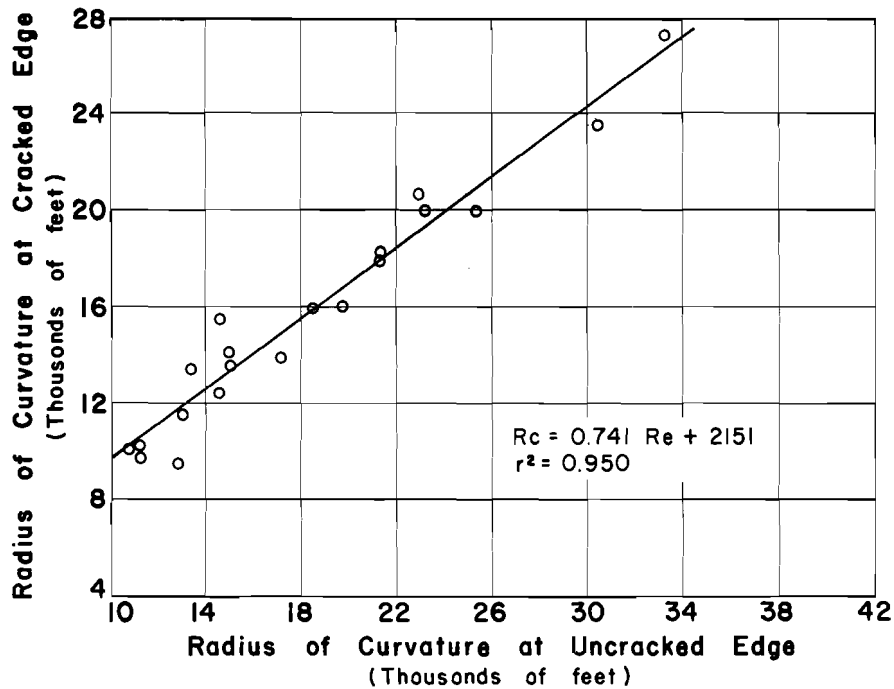
CRACKED EDGE VS. UNCRACKED
EDGE RADIUS OF CURVATURE

SUMMER

Figure 4.16
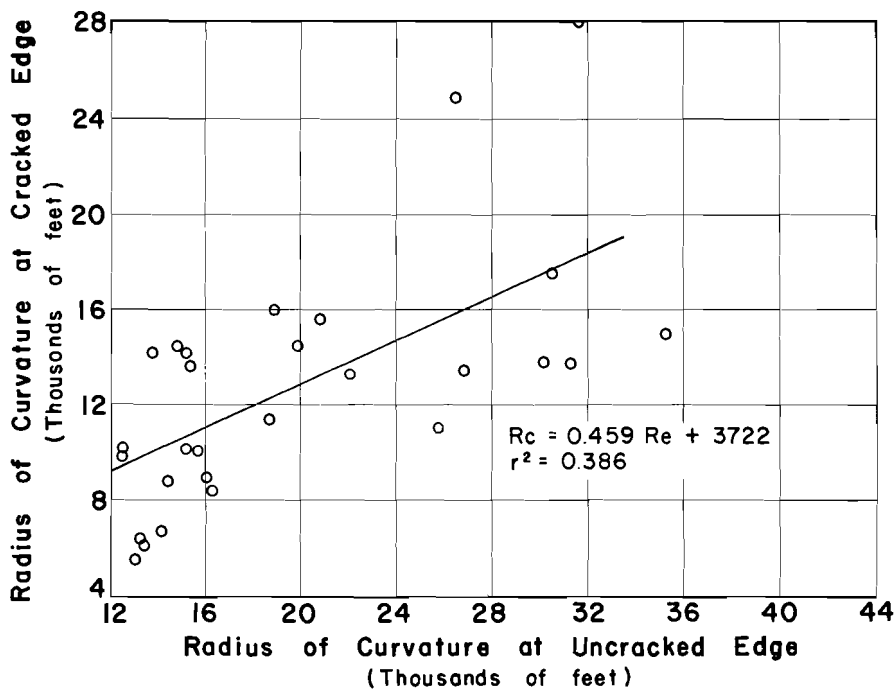
CRACKED EDGE VS. UNCRACKED
EDGE RADIUS OF CURVATURE

SPRING

Figure 4.17

were taken and the general moisture condition of the soil.

Season. Data was taken on a statewide basis in each
of the four seasons of the year. The deflection and
radius of curvature data taken during these four seasons
were analyzed by comparing each set of data to that taken
during the summer. The comparison showed only whether the
deflections and stresses were more or less in the fall,
winter, and spring than in the summer. In Figure 4.18
these comparisons showing more or less deflection than the
summer data are expressed as percentages. The results
indicate that the deflections during fall and winter were
generally greater than the summer, whereas, the spring
deflections were significantly smaller than the summer.
Thus the deflection might in some way be related to the
season; however, for the fall and winter there was not
very much difference in the data.

The results of the stress analysis shown in Figure
4.19 show that the seasonal comparisons with the summer
data are consistent in showing that the pavements ex-
perience less stress in the summer than during the other
seasons.

Soil Moisture Condition. Each time data was taken
on a test section, the general environmental conditions
of the soil adjacent to the roadway in a hole one foot
deep was classified as dry, moist or wet. As far as the
moisture effects are concerned, it was found that the
fourth data run which was the spring run, measured
deflections which were much less. During the entire
spring run general rains were experienced over the state.
Of the four runs, the spring run was by far the wettest
of the four runs.

SEASONAL COMPARISON OF DEFLECTION

FIGURE 4.18

PERCENT OF COMPARISONS SHOWING MORE OR LESS
STRESS THAN DURING SUMMER
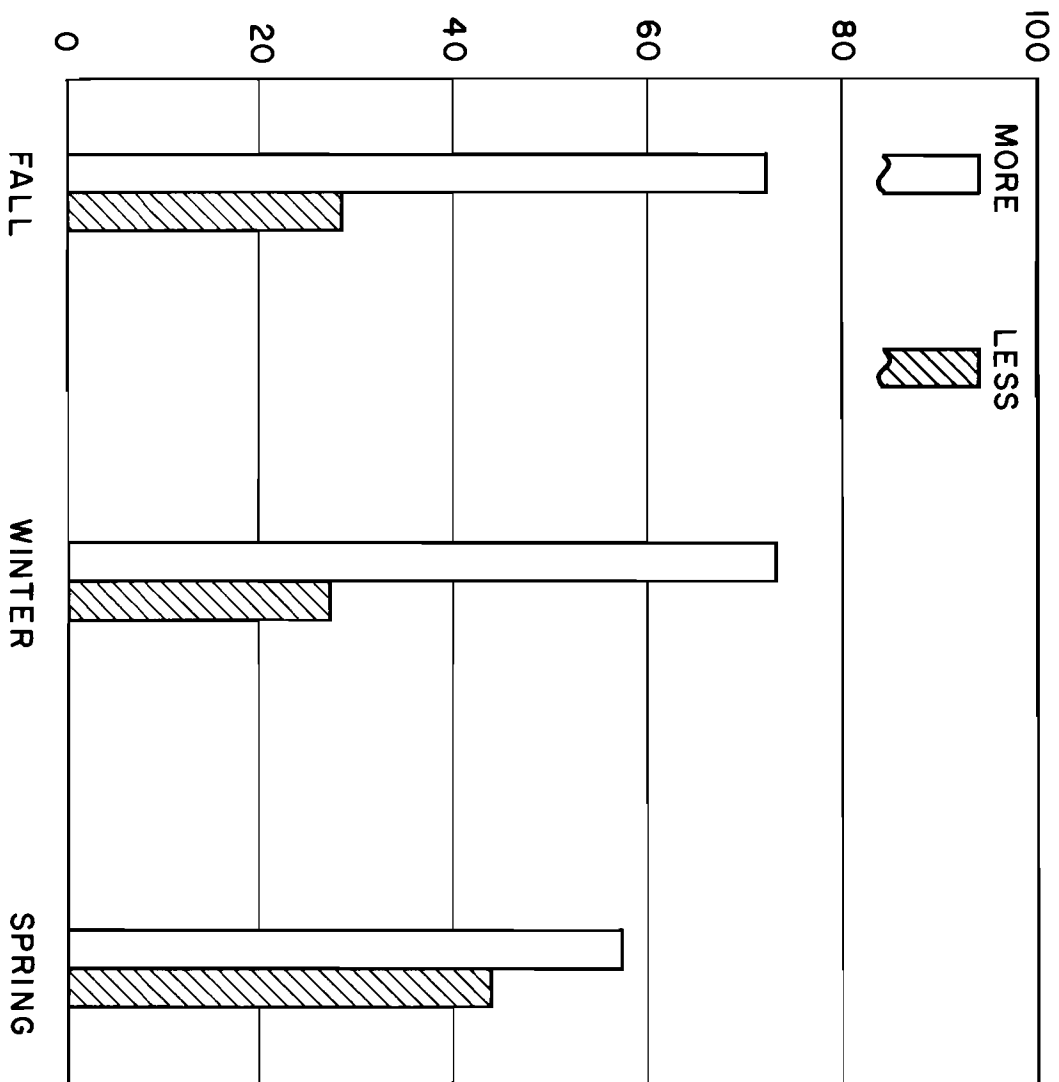
SEASONAL COMPARISON OF STRESS

FIGURE 4.19

V. CORRELATION OF VARIABLES

Deflection

The variables studied herein that affect deflection are the crack spacing, surface crack width, concrete modulus of elasticity and modulus of rupture, pavement slab thickness, pavement type, strength characteristics of the subgrade and subbase, and moisture conditions. With the exception of the semi-controlled variables and the modulus of rupture, these variables will be correlated into an equation in this Chapter.

A model equation was developed which encompassed the variables to be correlated. The model was based on previous work and also on work done at the AASHO Road Test.[5, 8] The model chosen to relate the variables is basically an extension of the Road Test model and is of the following form:

$$D_c = \frac{A_o \, L \, 10^{B_5 \frac{\Delta x}{\bar{X}}} \, \bar{X}^{B_4}}{D^{1.75} \, E^{B_2} \, SS^{B_3} \, 10^{0.0147 \, T}} \quad (5.1)$$

Where:

L = Load in kips
$\underline{x}$ = Surface crack width in inches
$\bar{X}$ = Average crack spacing in feet
D = Slab thickness in inches
E = Concrete modulus of elasticity, psi.
SS = Soil support
D_c = Deflection at crack position, inches
D_e = Deflection at midspan position, inches
T = Temperature differential between top and bottom of the slab, °F.

A_o, B_1, B_2, B_3, B_4, and B_5 are constants determined from a regression analysis on the data.

Slab thickness was not truly a full factorial variable consequently it could not be entered as an independent variable and had to be analyzed separately. All the subsequent regression analyses were performed for the eight inch pavement thickness factorial. The 1.75 power for the thickness term will be established later in the report.

The soil support term is a combination of the subgrade and subbase strength characteristics. The soil support is a calculated value which was developed in a previous analysis. In some cases the natural soil was stabilized with lime (generally clay) to facilitate construction operations by providing a working platform. These cases required a special handling as outlined in Appendix F.

The soil support is defined as:

$$SS = \left(\frac{U_1 + U_2}{T_{sg}} \right)^{1/4} \qquad (5.2)$$

Where:

SS = Soil support

U = Unconfined compressive strength of subbase and subgrade materials in psi at an age of seven days

T_{sg} = Texas Triaxial classification of subgrade material

$1,2$ = subscripts denoting subbase and stabilized subgrade respectively

In all subsequent analysis the load, L, will be 18 kips and the pavement slab thickness will be eight inches. The linear form of load used here has been qualified in another report on this project[7] and studies by others[5]. The data from each run was carefully analyzed to screen out what might be considered erroneous.

The power term for the temperature differential term was derived in another report on this overall study.[8] The temperature differential, the pavement thickness, and the load terms were not a part of the full factorial experiment, but in order that their effect would be reflected in the A_O term. Constant values for the eight inch factorial were inserted into the equation for variables not considered in the semi-factorial experiment. The values inserted into the equation were an 18 kip single axle load, eight inches for pavement thickness, and zero for temperature differential. These factors were then considered as constant and moved to the left of the equation.

A multiple regression analysis was made by use of the 1604-A Control Data Computer on each data run for deflection at the crack position, D_c, and also for deflection midway between cracks, D_e. The constants and the statistics derived from the regression analysis of each of the four runs are shown in Table 5.1, Computed Constants and Statistics.

The calculated deflection was plotted against the measured deflection for each data run and for each load position. These graphs are shown in Figures 5.1 through 5.8. Note the same general pattern for runs 1, 2 and 3 for both the crack and midspan deflections. The deflections at both crack and midspan were very small on Run 4, as discussed previously, when compared to the three previous data runs.

In Table 5.1 note that several values of B_4 are negative. This same result was the case in a previous analysis.[8] The crack spacing deflection relationship is bowl-shaped curve which is concave upwards. When the crack spacing is greater than that at the point of zero slope, B_4 is positive and when it is smaller B_4 is negative. Figure 5.9 is an example of the deflection-crack spacing relationship that results in a change of signs on B_4.

Several of the values calculated for B_2 are also negative. B_2 is the exponent on the modulus of elasticity

TABLE 5.1

COMPUTED CONSTANTS AND STATISTICS

FROM REGRESSION ANALYSIS*

COMPUTED VALUES / DATA RUN / LOAD POSITION		A_0	B_2	B_3	B_4	B_5	r	r^2	σ
CRACK	1	6.664	0.334	0.681	−0.060	3.222	0.698	0.487	± 0.0032
	2	0.00256	−0.123	0.526	0.1100	13.437	0.551	0.303	± 0.0029
	3	0.1220	0.104	0.690	0.0900	13.911	0.662	0.438	± 0.0030
	4	0.1099	0.1249	0.6869	0.0794	13.575	0.694	0.482	± 0.0021
MIDSPAN	1	0.0118	−0.0684	0.3211	−0.1938	7.816	0.407	0.166	± 0.0035
	2	0.0726	0.0418	0.3434	−0.3294	7.055	0.244	0.060	± 0.0032
	3	0.00373	−0.124	0.8709	0.1814	11.798	0.733	0.538	± 0.0027
	4	0.0749	0.1026	0.7179	0.1897	4.876	0.515	0.265	± 0.0031

r = COEFFICIENT OF CORRELATION
r^2 = COEFFICIENT OF DETERMINATION
σ = STANDARD ERROR OF ESTIMATE

* FOR EQUATION 5.1
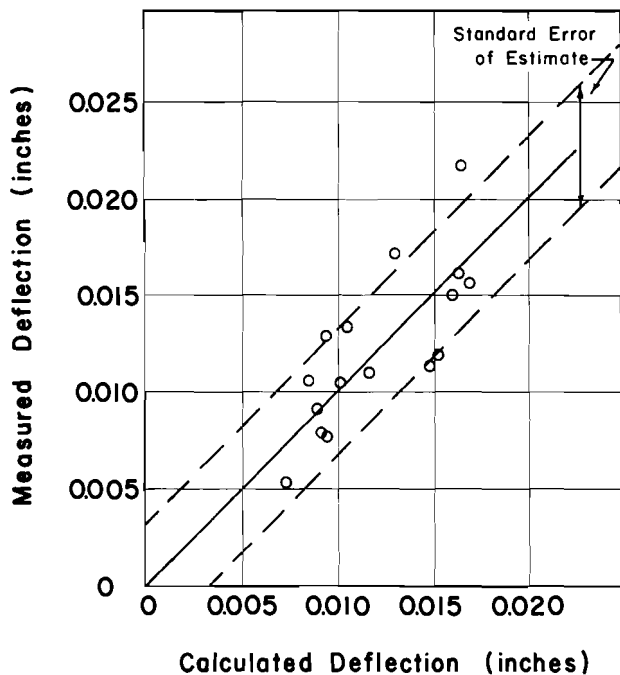
MEASURED vs. CALCULATED
DEFLECTION AT CRACKED EDGE
FALL
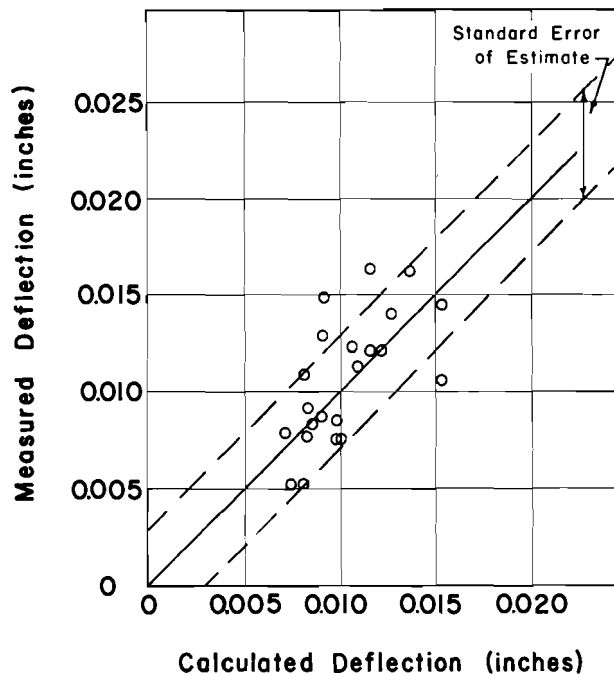
Figure 5.1

MEASURED vs. CALCULATED
DEFLECTION AT CRACKED EDGE
WINTER

Figure 5.2
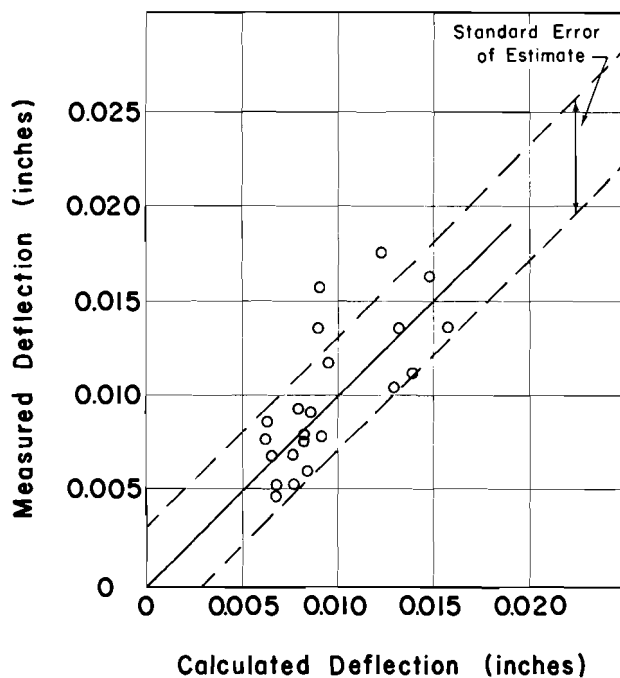
MEASURED vs. CALCULATED
DEFLECTION AT CRACKED EDGE
SUMMER

Figure 5.3
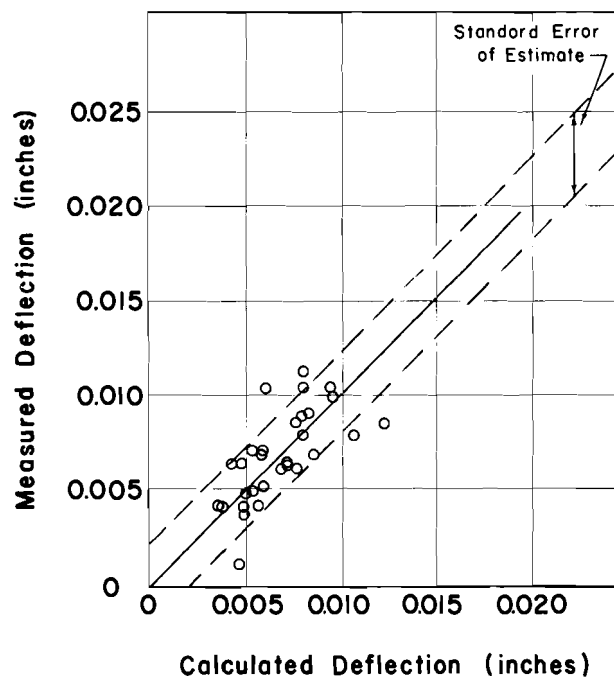
MEASURED vs. CALCULATED
DEFLECTION AT CRACKED EDGE
SPRING

Figure 5.4
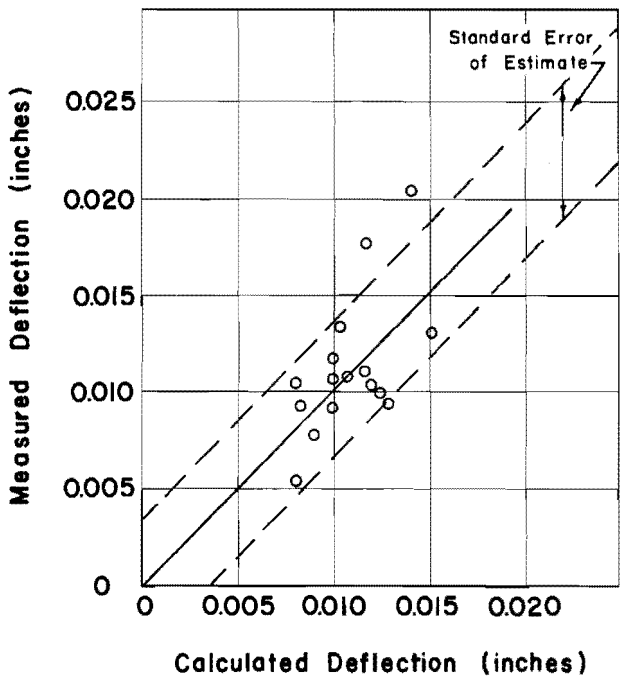
MEASURED vs. CALCULATED
DEFLECTION AT UNCRACKED EDGE
FALL

Figure 5.5
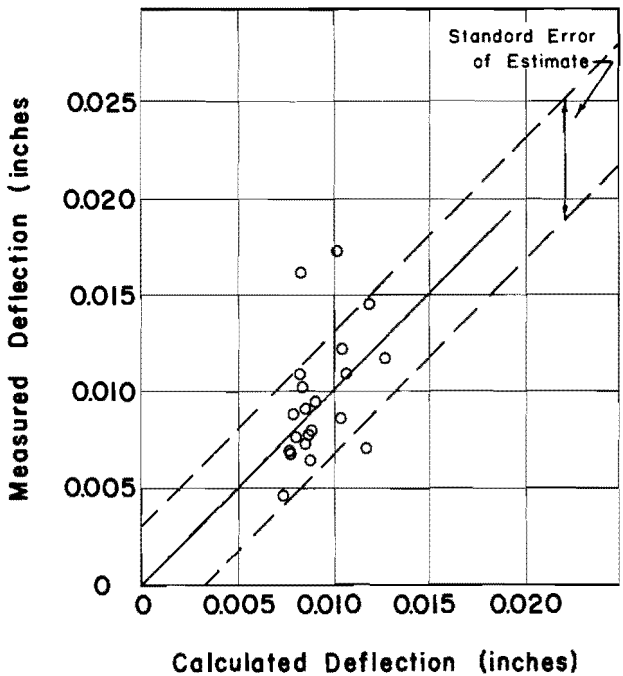
MEASURED vs. CALCULATED
DEFLECTION AT UNCRACKED EDGE
WINTER

Figure 5.6
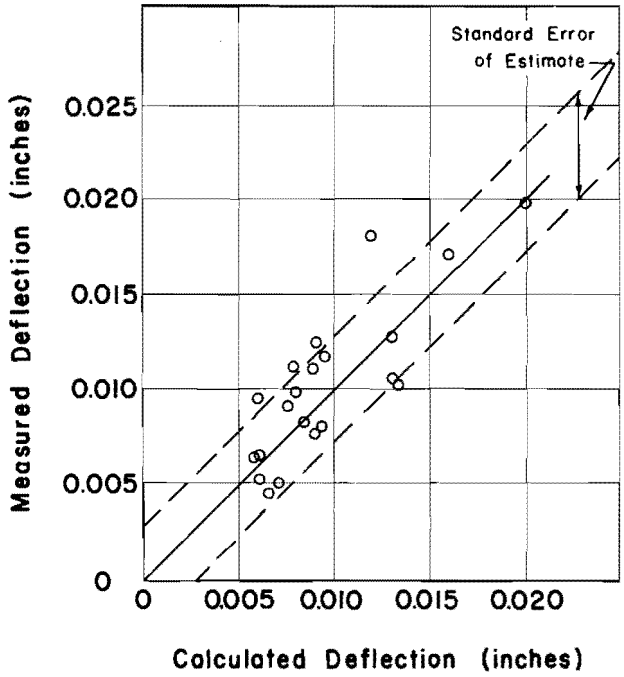
MEASURED vs. CALCULATED
DEFLECTION AT UNCRACKED EDGE
SUMMER

Figure 5.7
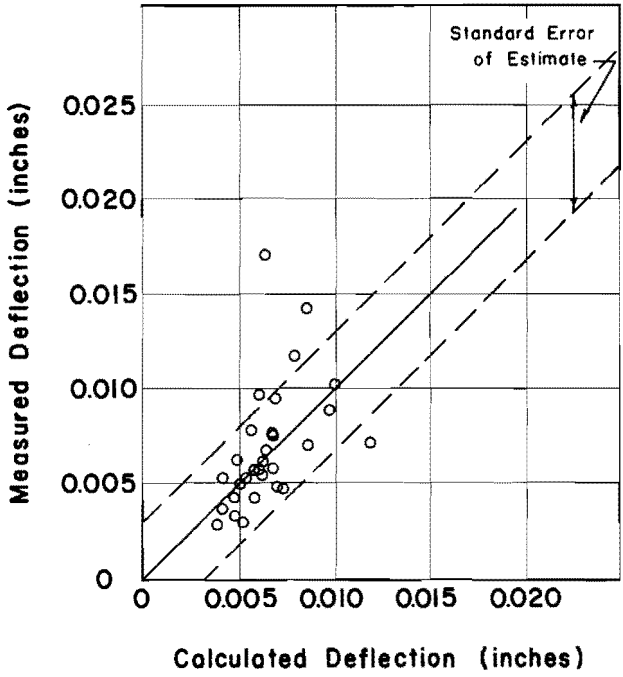
MEASURED vs. CALCULATED
DEFLECTION AT UNCRACKED EDGE
SPRING

Figure 5.8
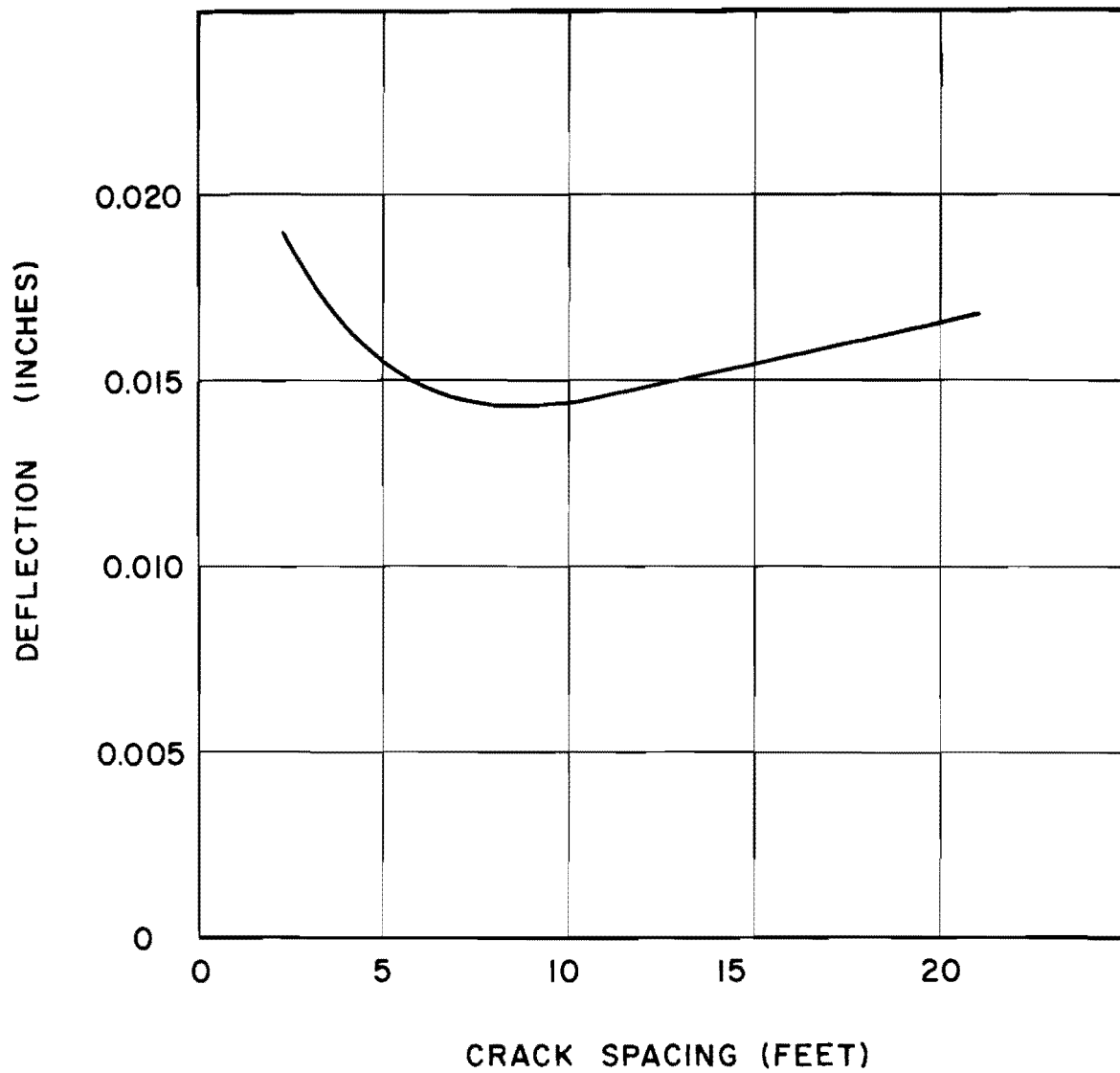
DEFLECTION VERSUS CRACK SPACING

FIGURE 5.9

term in the model equation. A negative B_2 would be in disagreement with theoretical concepts. Earlier in this chapter it was pointed out that the low modulus of elasticity CRCP was deflecting less than the high modulus of elasticity CRCP. Another investigation on an experimental CRCP showed this same factor between lightweight and conventional aggregate concrete.[7]

Note that the constants for each variable term generally have approximately the same magnitude, with only a few exceptions. The data from the first three runs were comparable, therefore, it was combined and a regression analysis was run on it. This resulted in two final equations, one for deflection at the crack position and another for deflection at a point midway between cracks. The computed constants and statistics are shown in Table 5.2. The equation would be applicable to a dry condition, for a wet condition the equation for Run 4 would be used. Note that the standard error is only slightly greater than the resolution of the Benkelman Beam.

Radius of Curvature

The radius of curvature data has been examined thus far in terms of stress, but the subsequent analysis will be in terms of the radius of curvature data.

The variables that were investigated that might affect the radius of curvature are the average crack spacing, soil support, concrete modulus of elasticity, load, and slab thickness. Thus radius of curvature is some function of all these variables.

$$R_c, R_e = f \; (\overline{X}, \; SS, \; E, \; L, \; D)$$

Where: R_c = Radius of curvature at crack position
          R_e = Radius of curvature at midspan position
          All other terms have been defined previously.

A model equation for radius of curvature was logically derived using the same concept as developed in the deflection equation.

TABLE 5.2

COMPUTED CONSTANTS AND STATISTICS FOR DEFLECTION EQUATIONS

| | REGRESSION ANALYSIS COMPUTATIONS | | | | | | | |
	A_0	B_2	B_3	B_4	B_5	Coefficient of Correlation	Coefficient of Determination	Standard Error of Estimate
CRACK	0.3779	0.1683	0.6513	0.0266	6.3407	0.6971	0.486	±0.0028
MIDSPAN	0.1362	0.0977	0.5601	-0.0462	4.1266	0.5544	0.307	±0.0033

The following is the model with the variables considered:

$$R_c = \frac{A_o\ D^{1.75}\ E^{B_2}\ SS^{B_3}\ \bar{X}^{B_4}}{L} \qquad (5.3)$$

Where all terms are as previous defined.

In the radius of curvature study the slab thickness again could not be entered as an independent variable due to a shortage of test sections on pavement thinner than eight inches. Thus the same thickness term was used here as in the deflection analysis, $D^{1.75}$.

Although the crack width and temperature differential are not reflected in Equation (5.3), they were considered in this study and previous studies. Previous studies indicated that the effect of temperature differential on the radius of curvature was very slight or non-existant. Therefore, on this basis, the temperature differential term was deleted. In regard to crack width, this term was included in the equation, but was found that the statistics of correlation were improved by deleting it from the regression equation.

The radius of curvature of the CRCP is studied at two points on the continuous slab, across the volume change crack and midway between the cracks. The crack radius of curvature was analyzed for each data run except the fourth data run. The individual data runs were analyzed using multiple regression techniques. The regression constants for the model equation are shown in Table 5.3. In order to obtain a more general equation for the radius of curvature at the crack position, the field data was examined and Runs one and two were combined to form the data for the regression which would produce the final equation for radius of curvature at the crack position. Figures 5.10 through 5.13 show the measured radius of curvature plotted against the calculated radius of curvature for the crack position for Runs one, two, and three and the combined data. The computed constants and the statistics for the final equation are shown in Table 5.4.

TABLE 5.3
COMPUTED CONSTANTS AND STATISTICS

RADIUS OF CURUATURE ANALYSIS *

		A_0	B_2	B_3	B_4	r	r^2	σ
CRACK	1	0.000832	0.9819	0.6572	−0.2623	0.9518	0.9059	±962
	2	350.5333	0.1548	0.3429	−0.1766	0.5574	0.3107	±1716
	3	53.4066	0.2898	0.4070	−0.0035	0.6900	0.4762	±2132
MIDSPAN	1	0.0742	0.7395	0.1882	0.0277	0.9527	0.9076	±868
	2	1779.2667	0.0639	0.3102	0.0863	0.4368	0.1908	±2247
	3	313.4298	0.1736	0.5872	0.0345	0.7503	0.5630	±2798
	4	1337.6603	0.0832	0.2894	0.1147	0.4453	0.1983	±2525

(COMPUTED VALUES / DATA RUN / LOAD POSITION)

r = COEFFICIENT OF CORRELATION
r^2 = COEFFICIENT OF DETERMINATION
σ = STANDARD ERROR OF ESTIMATE

* FOR EQUATION 5.3
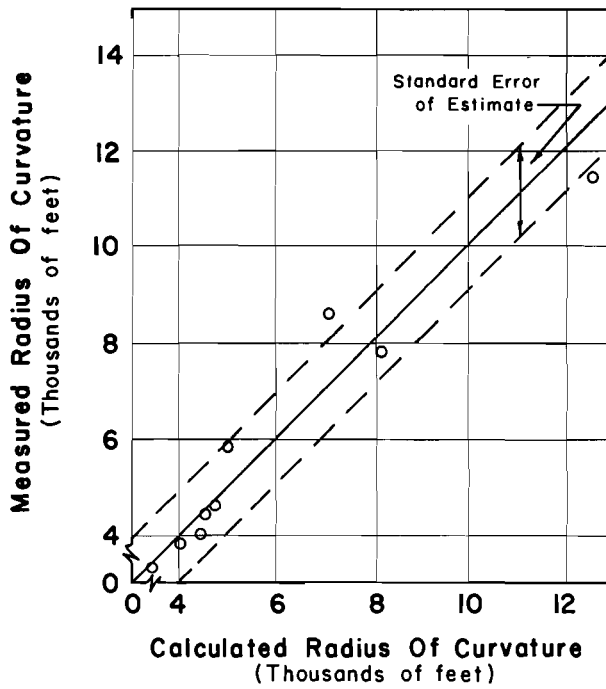
MEASURED vs. CALCULATED RADIUS
OF CURVATURE AT CRACKED
EDGE – FALL

Figure 5.10
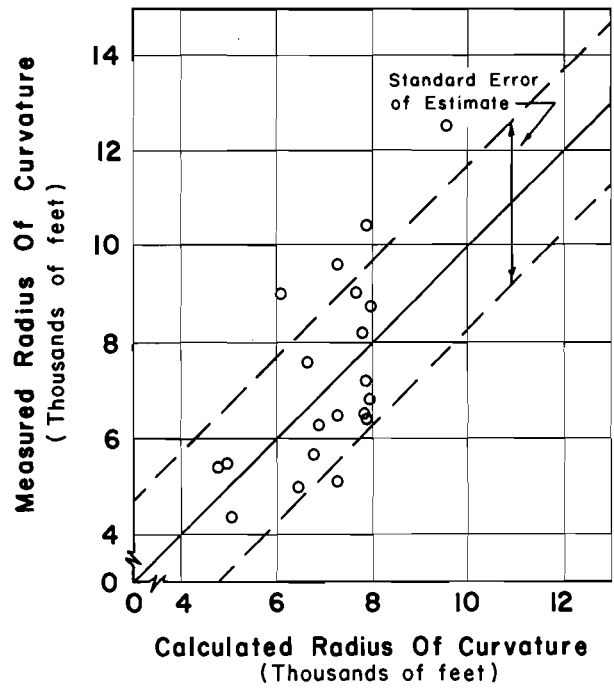
MEASURED vs. CALCULATED RADIUS
OF CURVATURE AT CRACKED
EDGE – WINTER

Figure 5.11
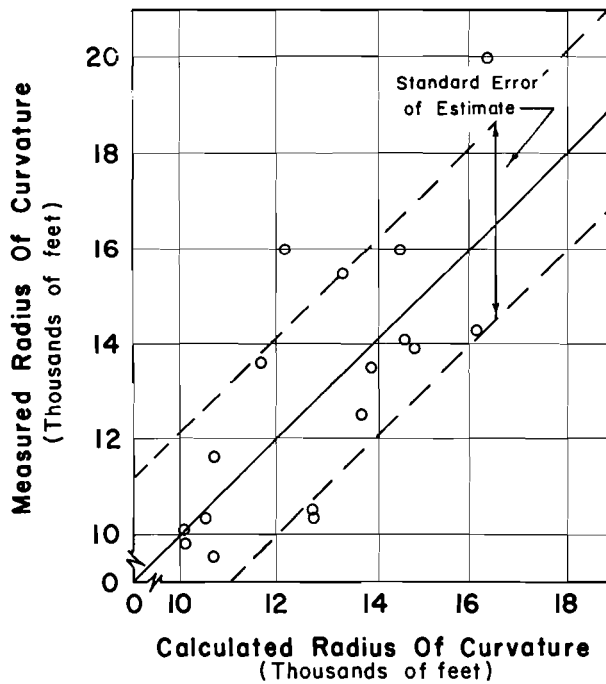
MEASURED vs. CALCULATED RADIUS
OF CURVATURE AT CRACKED
EDGE – SUMMER

Figure 5.12
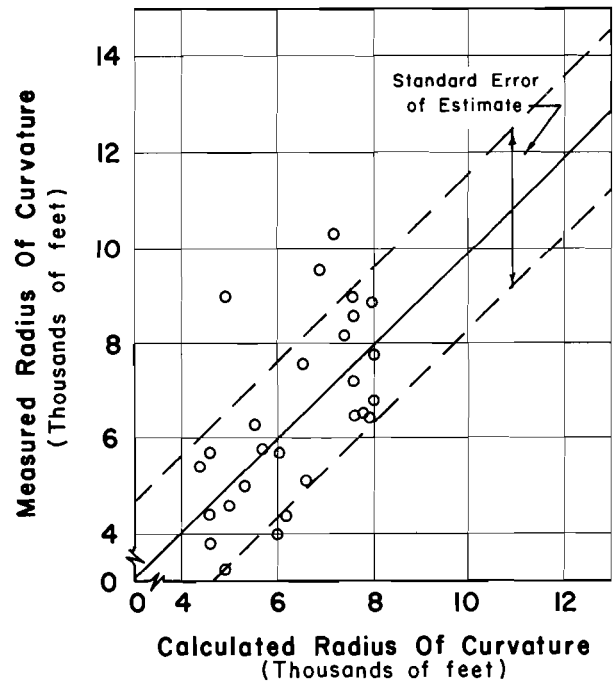
MEASURED vs. CALCULATED RADIUS
OF CURVATURE – COMBINED DATA

Figure 5.13

The midspan radius of curvature data was analyzed in like manner as the crack radius data; however, here all four data runs were used to relate the parameters studied to radius of curvature. The computed constants and statistics for the four equations are shown in Table 5.4. Figures 5.14 through 5.17 show the calculated radius of curvature plotted against the measured midspan radius of curvature.

TABLE 5.4

COMPUTED CONSTANTS AND STATISTICS FOR RADIUS OF CURVATURE EQUATIONS

	REGRESSION ANALYSIS COMPUTATIONS						
	A_0	B_2	B_3	B_4	Coefficient of Correlation	Coefficient of Determination	Standard Error of Estimate
CRACK	15.3039	0.3312	0.5467	-0.0772	0.6391	0.4085	±1617
MIDSPAN	333.3153	0.1729	0.3579	0.0909	0.5957	0.3548	±2508
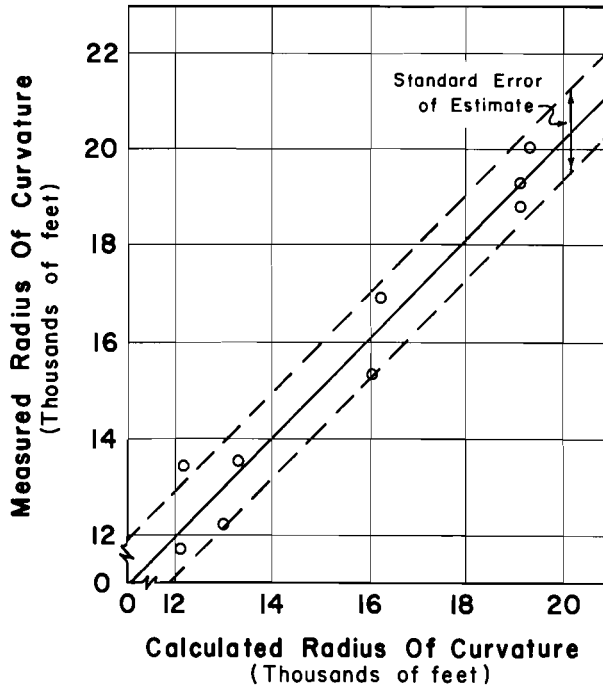
MEASURED vs. CALCULATED RADIUS
OF CURVATURE AT UNCRACKED
EDGE – FALL

Figure 5.14
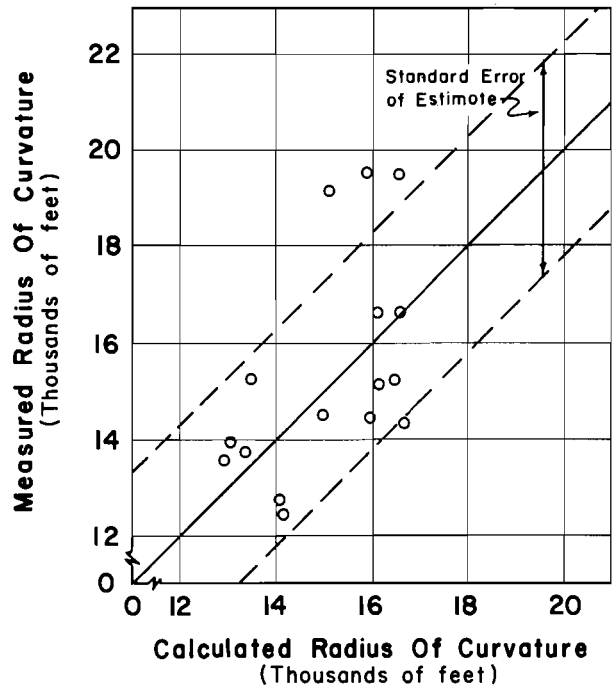
MEASURED vs. CALCULATED RADIUS
OF CURVATURE AT UNCRACKED
EDGE – WINTER

Figure 5.15
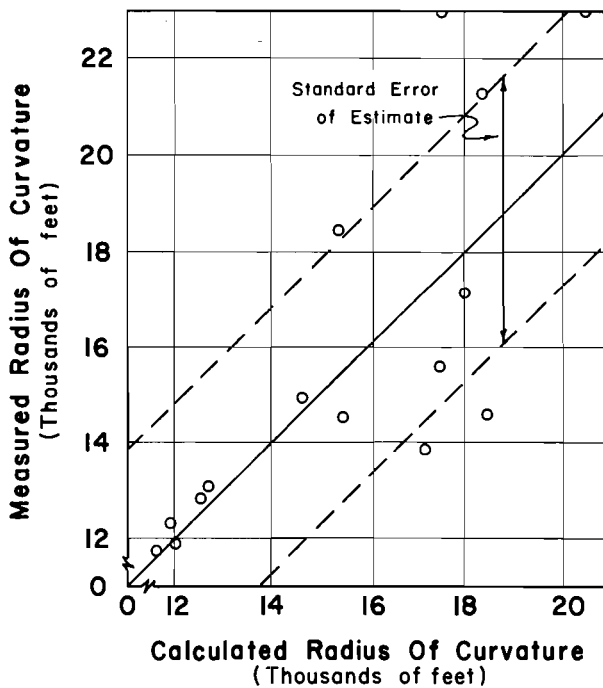
MEASURED vs. CALCULATED RADIUS
OF CURVATURE AT UNCRACKED
EDGE – SUMMER

Figure 5.16
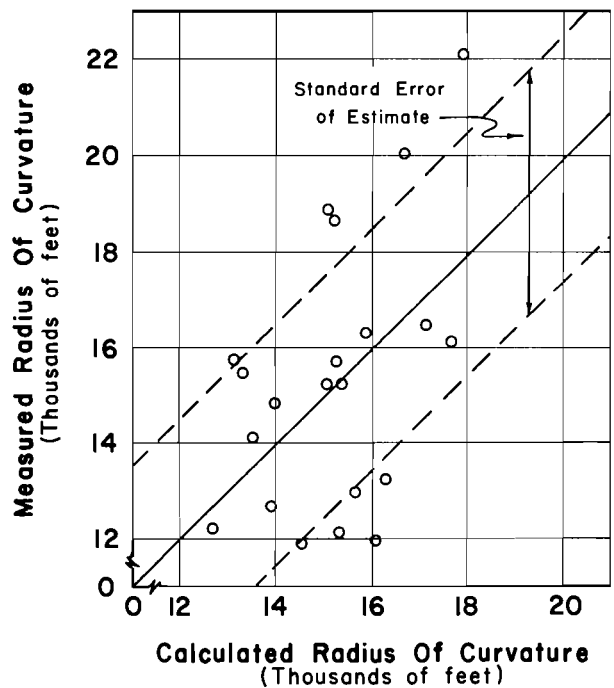
MEASURED vs. CALCULATED RADIUS
OF CURVATURE AT UNCRACKED
EDGE – SPRING

Figure 5.17

VI. DISCUSSION OF RESULTS

Deflection

In general, the control variables considered in this study were found to affect the deflection of a CRCP. Their effect follows a pattern which can be expressed by a mathematical expression. Of the semi-controlled variables considered, it was found that the soil moisture condition affected the deflection although the findings were contrary to the generally accepted criteria of greater deflection for a moist condition. In addition, the findings of this study tend to verify the assumptions used in the design and development of CRCP.

Soil Moisture. The four data runs were made in different seasons over a period of about two years. At the times the data were taken, the general soil moisture conditions were not the same. The fourth run was exceptionally wet, and deflections on this run were all considerably less than what they had been on the first three runs. Initially, this discrepancy between the findings and the normal assumption of more deflection for a wet condition caused much concern for errors which might have been made on the fourth run in taking the data. When the weather conditions were the same as on the fourth run, the pavement deflections on approximately one-third of the sections were measured again. As was the case previously, the deflections were small and for all practical purposes identical to those of the fourth run (see Appendix E).

It is now believed that when the subgrade and sub-base materials are saturated they respond to quick loading as does a soil sample in an undrained triaxial test. The load applied to the pavement is supported partially by the pore-water in the pavement foundation rather than the soil grains as is the case where the soil is not saturated.(13)

It should also be pointed out that the summer run
where the soil was the dryest, experienced slightly less
deflection than periods when the subsoil was partially
saturated. Of course, this latter condition could be
the result of smaller cracks due to summer temperatures.

Equations. The deflection equations derived herein
are extensions to the one developed in an earlier report.[8]
The previous equation was based on data taken from only
two test sections, and the ones herein are based on 20
pavements with three sets of data from each for the dry
condition and one set for the wet run. Table 6.1 gives
a comparison of the equations with the equation developed
in Research Report 46-4.[8] The earlier equation was
based on crack position data only.

Figures 6.1 through 6.2 were prepared to illustrate
the capability of the equation for predicting the observed
deflection. In each case, the regression equation developed
from the data for both the crack position and midspan
position was used to calculate the deflection for a given
set of conditions on a test section. This calculated
deflection was then compared against measured deflections
for the test sections as portrayed in the referenced
figures. Note the close agreement, in most cases, between
the measured and calculated values. In some cases, both
the measured and calculated deflection appear to be out
of line with what is to be expected, but these exceptions
are normally due to a lime stabilized subgrade and are
so marked on the figures. These figures are typical of
all runs, hence, these observations support the validity of
using these equations in design work.

Modulus of Elasticity. The findings in this study in
regard to the modulus of elasticity of concrete contradict
the generally accepted theory of a lower modulus of
elasticity slab deflecting more than a high modulus one
for equal conditions. Although the levels of the modulus
are not too far apart in magnitude, another experiment on
this same research project, wherein the levels were con-
siderably greater through the use of two entirely
different coarse aggregate types, indicated the same results.

TABLE 6.1

COMPARISON OF REGRESSION ANALYSIS CONSTANTS

CONSTANT	OVERNIGHT STUDY	STATEWIDE STUDY
A_0	0.0106	0.3779
B_2	—	0.1683
B_3	0.8503	0.6513
B_4	0.0994	0.0266
B_5	4.8997	6.3407

$$D_c = \frac{A_0 \quad L \quad 10^{\frac{B_5 \triangle X}{\bar{X}}} \quad \frac{B_4}{T_{sg}} \quad 0.25\ B_3}{\frac{1.75}{D} \quad \frac{B_2}{E} \quad \frac{0.25\ B_3}{U} \quad \frac{0.0147\ T}{10}}$$

FIGURE 6.1

MEASURED AND COMPUTED DEFLECTIONS ON HIGH
MODULUS OF ELASTICITY CONCRETE
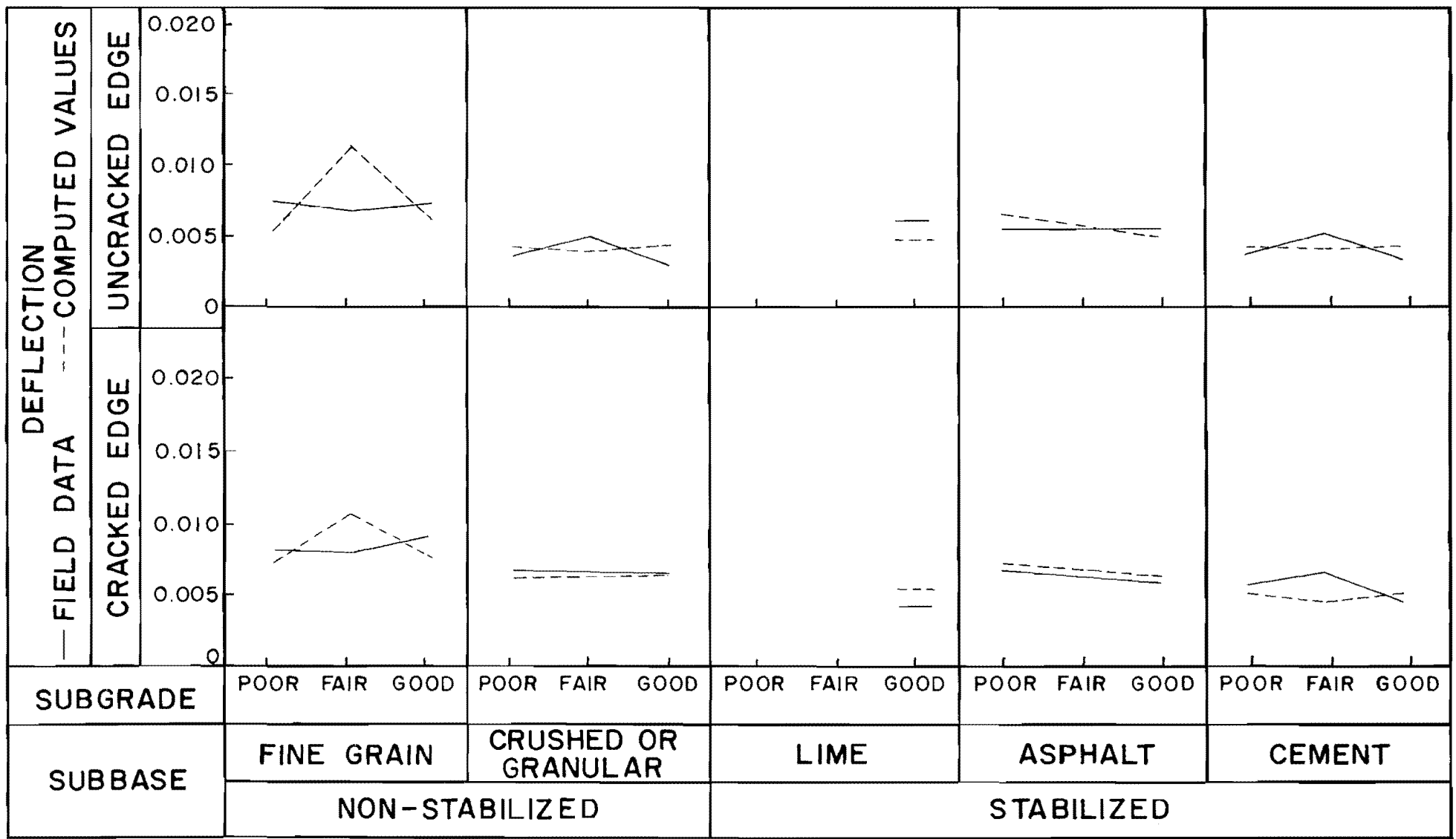
FIGURE 6.2

MEASURED AND COMPUTED DEFLECTIONS ON LOW MODULUS OF ELASTICITY CONCRETE
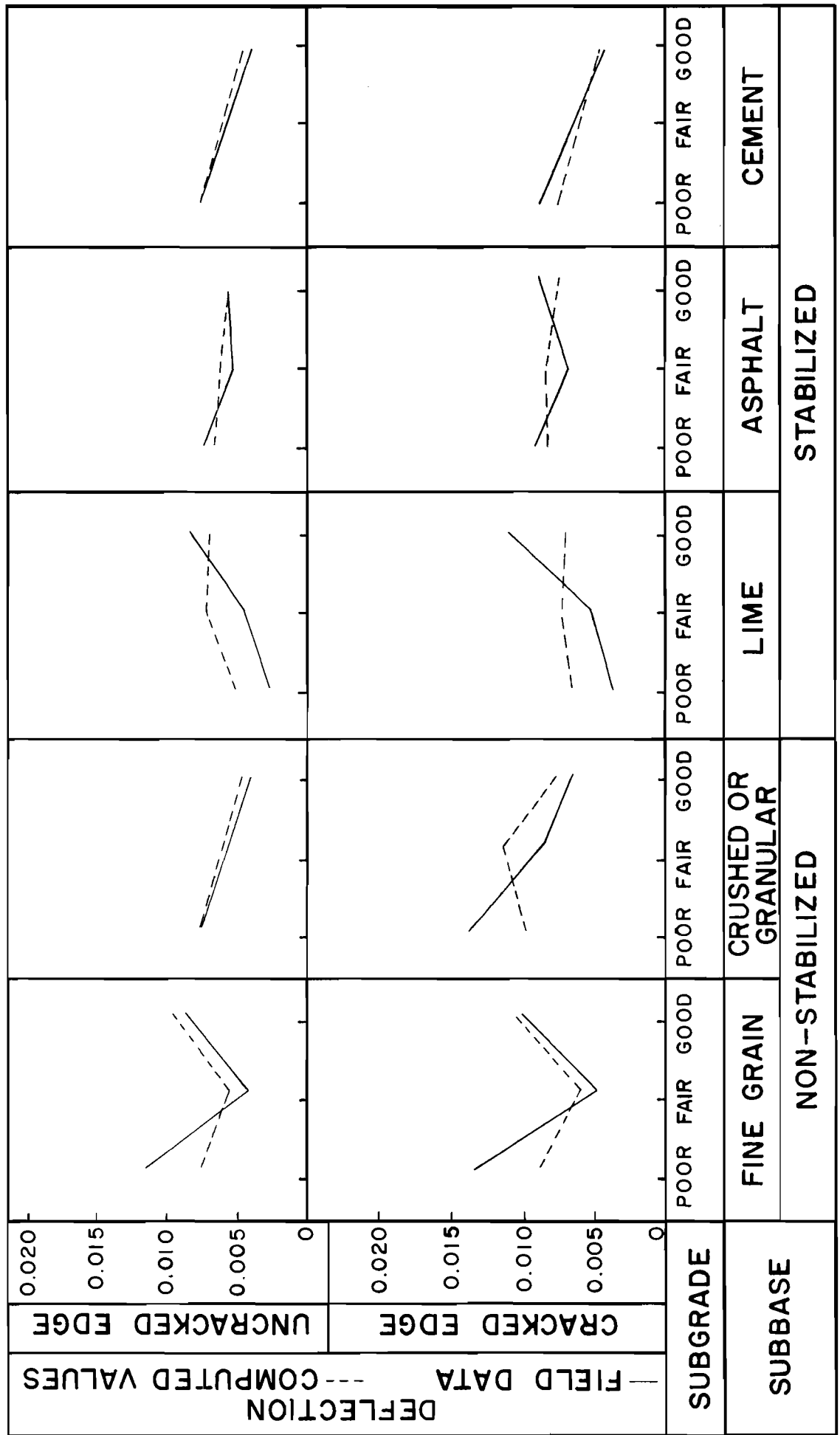
These two separate investigations along with a limited laboratory investigation lend credence to these observations of less deflections with a lower modulus of elasticity concrete.[14] It should be emphasized although that this observation can only be related to CRCP at this time, and should not be translated to JCP which may react differently.

There is a good possibility that this controversial observation attributed to modulus of elasticity could be an indirect effect of a combination of variables not considered in this experiment.

It may be hypothesized that generally speaking, a low modulus of elasticity concrete has a lower coefficient of thermal expansion. In this case the transverse volume change cracks would be smaller, hence, a greater degree of load transfer would be available. Therefore, with a greater load transfer less deflection would be experienced.

Furthermore, in the normal theoretical analyses of this condition, such as Westergaard, Pickett, Spangler, etc., the basic assumption is made that the subgrade reaction forces are vertical. An actual pavement on a subgrade deflecting under a wheel load develops a complicated interaction of shear forces and vertical forces which may result in these field observations rather than these developed in a simplified theoretical approach.

Final Equation. The equations developed contain the term soil support which was defined in Chapter Five by Equation 5.2. The soil support term can be eliminated from the deflection equations by substitution of Equation 5.2 into Equation 5.1. The dry or partially saturated condition was used as the level for selecting the final equation. Thus the equation for deflection takes the form:

$$Dc = \frac{0.3779 \; L \; 10^{\frac{6.3407 \, \triangle X}{\overline{X}}} \; 0.0266 \; Tsg^{0.1628}}{D^{1.75} \; E^{0.1683} \; (U_1 + U_2)^{0.1628} \; 10^{0.0147 \, T}}$$

Where all terms are as previously defined.

Radius of Curvature

The radius of curvature data shows that the average radius of curvature at the cracked edge for all data is about 52 per cent less than the radius of curvature at the uncracked edge. The radius of curvature at the crack and midspan was correlated by linear regression analysis for each of the four data runs, the graphs for which are shown in Figures 4.14 and 4.17.

Figures 6. 3 and 6. 4 show calculated and measured radius of curvatures plotted against the subgrade classifications for each subbase material type that was available.

Final Equation. The radius of curvature equations determined for combined data in Chapter Five contained the soil support term. Here again, the definition of soil support can be substituted and the radius of curvature equation will then take the form:

$$Rc = \frac{15.3039 \; D^{1.75} \; E^{0.3312} \; (U_1 + U_2)^{0.1367}}{L \; Tsg^{0.1367} \; \bar{X}^{0.0772}}$$

Where all terms are as previously described.

An attempt was made to add the crack width as another variable but the results were such that it would be better not to include the crack width.

Accuracy of Regression Equations

Nineteen sets of deflection and radius of curvature data were analyzed each by multiple regression methods. For each analysis a value of "r", the correlation coefficient was obtained. These values of "r" were checked against a table for their significance for the number of points and

FIGURE 6.3

MEASURED AND COMPUTED RADIUS OF CURVATURES
ON HIGH MODULUS OF ELASTICITY CONCRETE
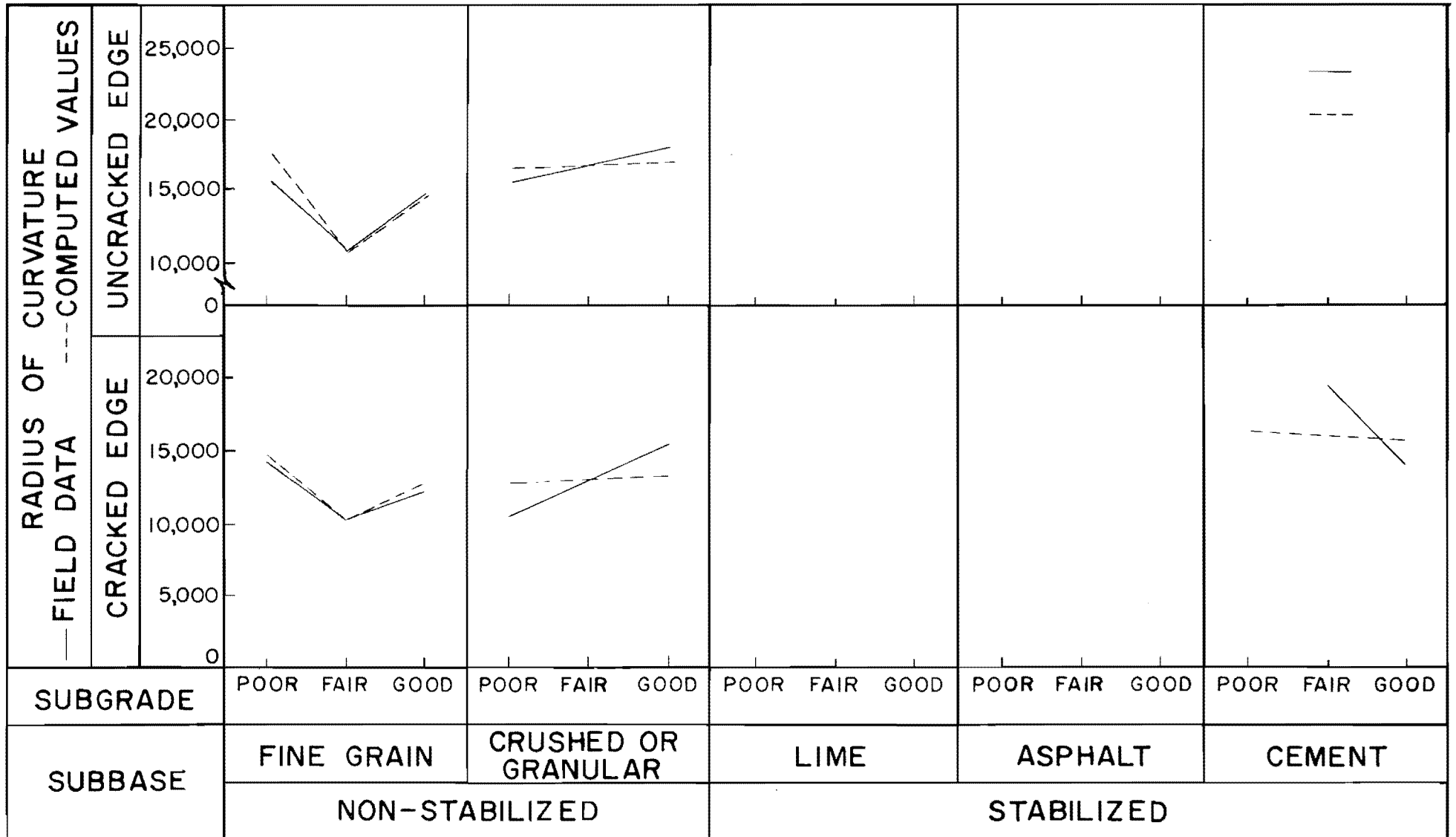
FIGURE 6.4

MEASURED AND COMPUTED RADIUS OF CURVATURES
ON LOW MODULUS OF ELASTICITY CONCRETE
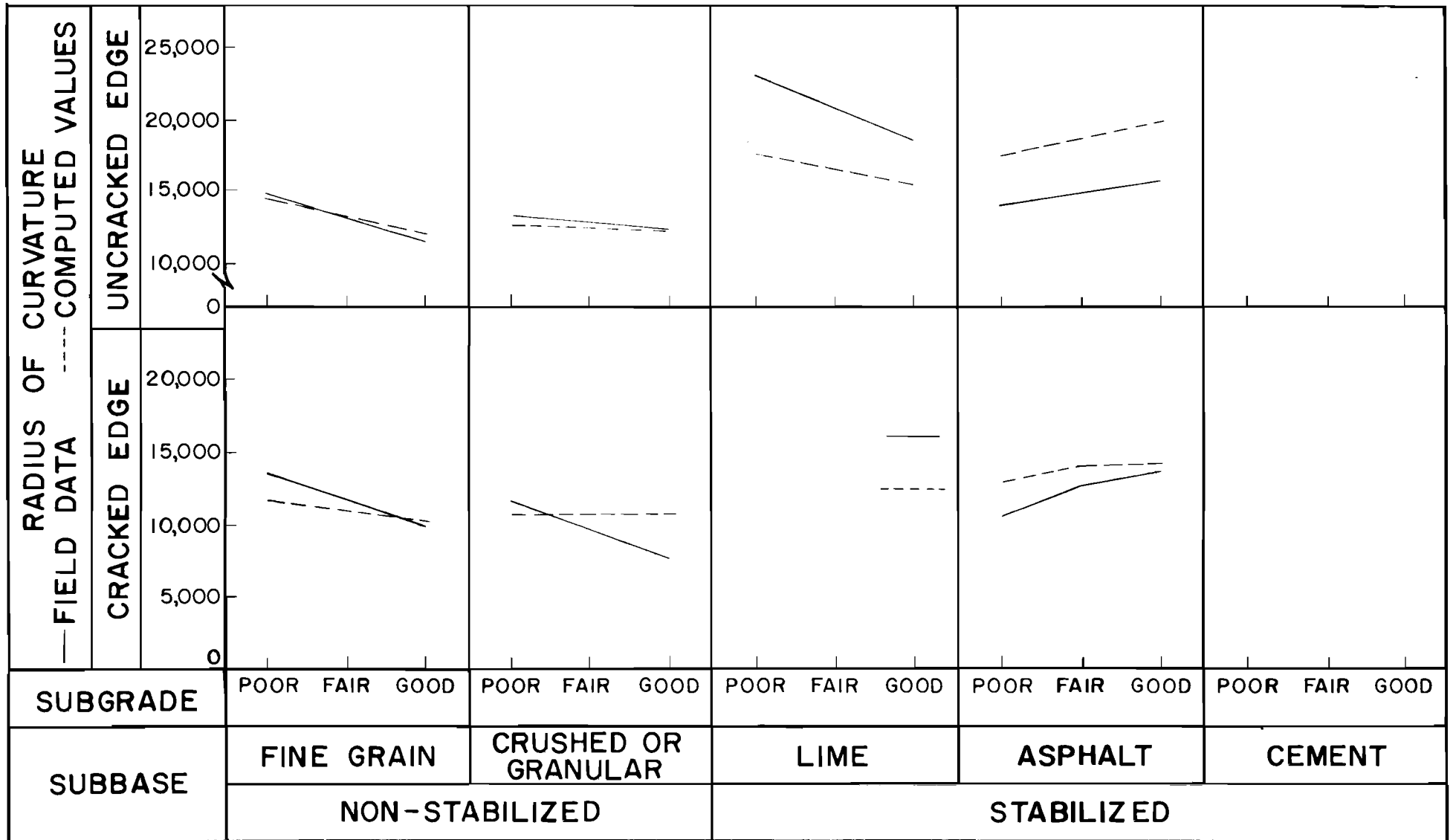
degrees of freedom.[15] Table 6.2 shows the results of the "r" check. A "G" indicates good and "F" indicates an "r" value less than that in the table.

The regression results appear to substantiate the form of the model equations. All checks on the correlation coefficients from the analysis of combined data were above that required to be significant. Previous discussions in an early chapter have shown the standard error of these equations is compatible with the accuracy of the equipment used. Thus the equations are in most cases statistically sound.

Validation of Design Assumptions

The findings of this study provides validity for the assumptions used in the original design analysis of CRCP. Two of these assumptions were outlined in the "Introduction". The equal magnitude of deflection at the crack position and midspan position indicates that sufficient granular interlock is provided so that approximately 100 per cent load transfer is experienced across a crack. This finding is applicable only where the pavements have 0.5 per cent longitudinal steel or more although there is a possibility that the lower limit on per cent steel may be less than the minimum used in this experiment. Considering these aspects, this finding is applicable over a wide range of support conditions and concrete properties and components.

Furthermore, the use of the Westergaard Interior Loading Conditions for determining the pavement thickness is a satisfactory procedure. The findings of this experiment indicate a two-inch differential between CRCP and JCP and is in agreement with field performance from a deflection standpoint. This finding also has validity over a wide range of support conditions and concrete properties.

Design Equations

The final equations presented herein for both deflection and radius of curvature provide an excellent criteria for developing equations to be used in the design of

TABLE 6.2

INVESTIGATING THE SIGNIFICANCE OF

CORRELATION COEFFICIENTS

ANALYSIS	CRACK	MIDSPAN
Deflection:		
Run 1	G	F
Run 2	G	F
Run 3	G	G
Run 4	G	G
Combined Data	G	G
Radius of Curvature:		
Run 1	G	G
Run 2	G	F
Run 3	G	G
Run 4		F
Combined Data	G	G

"G" – The coefficient of correlation is greater than a minimum value required for significance.

"F" – The coefficient correlation is less than a minimum value required for significance.

concrete pavements. Although there are numerous other
factors other than deflection and stress to consider in
the design of concrete pavements, this material will
present another excellent guideline for a designer to
use in selecting the final pavement structure design for
a given roadway.

Although per cent longitudinal steel and pavement
type are not enumerated in these design equations, they
may be inserted on the basis of other material and studies
developed in connection with this project. These equations
are empirical equations and care should be taken not to
extrapolate beyond the limits used in this analysis. The
following are some guidelines or boundary conditions which
should not be extrapolated beyond:

$$D_c = 0.003 \text{ inch to } 0.030 \text{ inch}$$
$$E = 3 \times 10^6 \text{ psi to } 6 \times 10^6 \text{ psi}$$
$$D = \text{six to eight inches for CRCP}$$
$$D = \text{eight to ten inches for JCP}$$
$$\overline{X} = \text{three to twelve feet}$$

VII. CONCLUSIONS

This deflection study of CRCP has encompassed a wide variety of conditions and a considerable part of the geographical area of the state. The study was conducted over a three year period and over 15,000 separate measurements of various types were used in this analysis. As a result of this field study and analysis, the following conclusions are warranted:

1. The variables studied herein that were found to affect the deflection of CRCP were concrete modulus of elasticity, modulus of rupture, crack spacing, surface crack width, pavement slab thickness, pavement type, strength characteristics of the subgrade and subbase, and the subsurface moisture conditions. An empirical equation was derived using these variables with the exception of modulus of rupture and moisture condition to predict the deflection of a continuously reinforced concrete pavement under a given wheel load.

2. An equation was also derived from the study that predicts the radius of curvature of a pavement, i.e., related to pavement stress in terms of the same variables with the exception of crack width.

3. It is recommended that the final equations derived herein be used to develop a nomograph predicting the deflection and radius of curvature for the variables studied. Through the use of this nomograph along with a maximum allowable deflection, pavements may be designed and/or checked in terms of the conditions existing on each project.

4. For the design equation mentioned above, the variables of pavement type and per cent longitudinal steel may be added to the equation on the basis of the studies herein and previous studies made in connection with this research project.

5. For continuous pavements, longitudinally reinforced with 0.5 per cent steel or greater, it was found

under a wide variation of support and environmental
conditions that the transverse cracks in CRCP are small
enough to retain sufficient aggregate interlock to main-
tain approximately 100 per cent load transfer across the
crack.

6. The transverse cracks were found to affect the
continuity of a CRCP since measurements indicated that
the radius of curvature was smaller, i.e., greater stress
at the crack than at a midspan point between cracks.

7. From a deflection and stress standpoint, pavements
with stabilized subbases are superior in performance to
pavements with non-stabilized subbases. All three of
the stabilizing agents considered in this study were found
to give excellent performance from a deflection standpoint,
but as a result of other studies that will be presented
in the future, it is recommended that lime stabilized sub-
bases be protected with a non-errosive material.

8. From a deflection standpoint, the present practice
of using a two-inch thinner pavement for CRCP in relation
to JCP as indicated by current design procedures is
correct and conservative. For a given set of conditions,
it was found that the deflection for an eight inch CRCP
is equal to or less than a ten inch JCP.

9. This study indicated that a reduction in thickness
for CRCP had slightly more effect on deflection than an
equal reduction in thickness for jointed pavement as found
at the AASHO Road Test. Although there is a slight
variation, the effect of pavement thickness on deflection
was found by (1) this study, (2) the AASHO Road Test, and
(3) Westergaard's theoretical analysis are in approximately
the same range.

10. The use of a lime stabilized subgrade, as prac-
ticed in Texas, for a working platform or moisture control,
was found to give an additional benefit of substantially
reducing the deflections of a continuous pavement. Under
certain conditions, the supporting characteristics of this
layer may be considered in design.

11. From a deflection and stress standpoint, the design details persently being used by the Texas Highway Department for CRCP appear to be more than adequate for the conditions found in Texas.

12. This study developed two findings that contradict widely accepted beliefs concerning deflection of concrete pavement, these being:

(a) It was found that pavement on moist or saturated foundations deflected less than when the support was dry or partially saturated. These observations were confirmed during two different wet periods and three dry periods.

(b) Although the difference is small, deflections and stresses are lower on low modulus CRCP than on high modulus concrete.

BIBLIOGRAPHY

1. "Status Report on Continuously Reinforced Concrete Pavement Built or Under Contract in the U.S.", Concrete Reinforcing Steel Institute, July, 1966.

2. Shelby, M.D. and McCullough, B.F., "Experience in Texas with Continuously Reinforced Concrete Pavement", Highway Research Board Bulletin 274, Washington, D.C.; National Academy of Sciences, January, 1960.

3. McCullough, B.F. and Ledbetter, W.B.,"LTS Design of Continuously Reinforced Concrete Pavements", Journal of the Highway Division, Proceedings of the ASCE, Vol. 86, No. HW4, December, 1960.

4. "AASHO Interim Guide for the Design of Rigid Pavement Structures", AASHO Committee on Design, April, 1962.

5. Highway Research Board, The AASHO Road Test, (Report No. 5, Pavement Research). Washington, D.C.; National Academy of Sciences, 1962.

6. McCullough, B.F., "Development of Equipment and Techniques for a Statewide Rigid Pavement Deflection Study", Research Report No. 46-1, Texas Highway Department, January, 1965.

7. McCullough, B.F., "Evaluation of Single Axle Load Response on an Experimental Continuously Reinforced Concrete Pavement", Research Report No. 46-3, Texas Highway Department, April, 1965.

8. McCullough, B.F. and Treybig, Harvey J., "Determining the Relationship of Variables in Deflection of Continuously Reinforced Concrete Pavement", Research Report No. 46-4, Texas Highway Department, August, 1965.

9. Manual of Testing Procedures, Volume 1, Texas Highway Department.

10. Design Manual for Controlled Access Highways, Texas Highway Department.

11. Standard Specifications for Road and Bridge Construction, Texas Highway Department, 1962.

12. Hudson, W.R., "Value of Single Load Response in Rigid Pavement Design", Paper presented at Texas Section ASCE, May 10, 1963.

13. Taylor, Donald W., Fundamentals of Soil Mechanics, (Ninth Printing, John Wiley & Sons, Inc., New York, 1956), pp. 381-392.

14. McCullough, B.F. and Mays, Ivan K., "A Laboratory Study of the Variables that Affect Pavement Deflection", Research Report No. 46-6, Texas Highway Department, August, 1966.

15. Snedecor, George W., Statistical Methods, (Ames, Iowa: Iowa State College Press, 1946), p. 351.

16. Westergaard, H.M., "Stresses in Concrete Pavements Computed by Theoretical Analysis", Public Roads, Volume 7, No. 2, April, 1926.

APPENDIX   A

Brief Description of Equipment

and

Experimental Procedure

EQUIPMENT AND EXPERIMENTAL PROCEDURE

At the outset of this study, a thorough investigation was made to determine what equipment was necessary for a statewide rigid pavement deflection study. Some existing equipment was investigated and used. Other equipment and procedures were developed by the Department for this project.

Some of the more vital pieces of equipment used in this investigation were the truck for load application, Benkelman Beams, Basin Beam, Microscope, and a portable temperature slab and recorder. This equipment is shown in Figures A.1 through Figure A.4.

Following is a brief description of each peice of equipment. For a detailed description and operational technique refer to reference six in the Bibliography.

Benkelman Beam. Two of the four beams had ten-foot probes, and the other two had eight-foot probes. The Benkelman Beams were positioned on the pavement in this study in a manner similar to that used at the AASHO Road Test. The beams were positioned at an angle of 30 degrees to the longitudinal edge of the pavement slab with the probe pointing toward the truck.[5] Figure A.1 shows a plan view of the position of the Benkelman Beam when taking measurements. On each test section, periodic measurements were made with several beams to insure that the reference feet of the measuring Benkelman Beams were not in the deflection basin.

Basin Beam. The Basin Beam, which is the instrument used to measure radius of curvature in terms of basin deflection, was designed by the Highway Design Division's Research Section and built by the shops of the Texas Highway Department. The placement of the Basin Beam when taking data is shown in Figure A.1. The probe of the dial gauge which is in the center of the beam is placed just to either side of the crack in the pavement.[6] The radius of curvature is computed using the geometrical relationship for three points on a circle.

Random Transverse Crack

Deflection Truck

ℂ of Pavement

20"

Basin Beam

1" 2"

Edge of Pavement

30°

10'

10'

Benkelman Beam

Edge of Shoulder
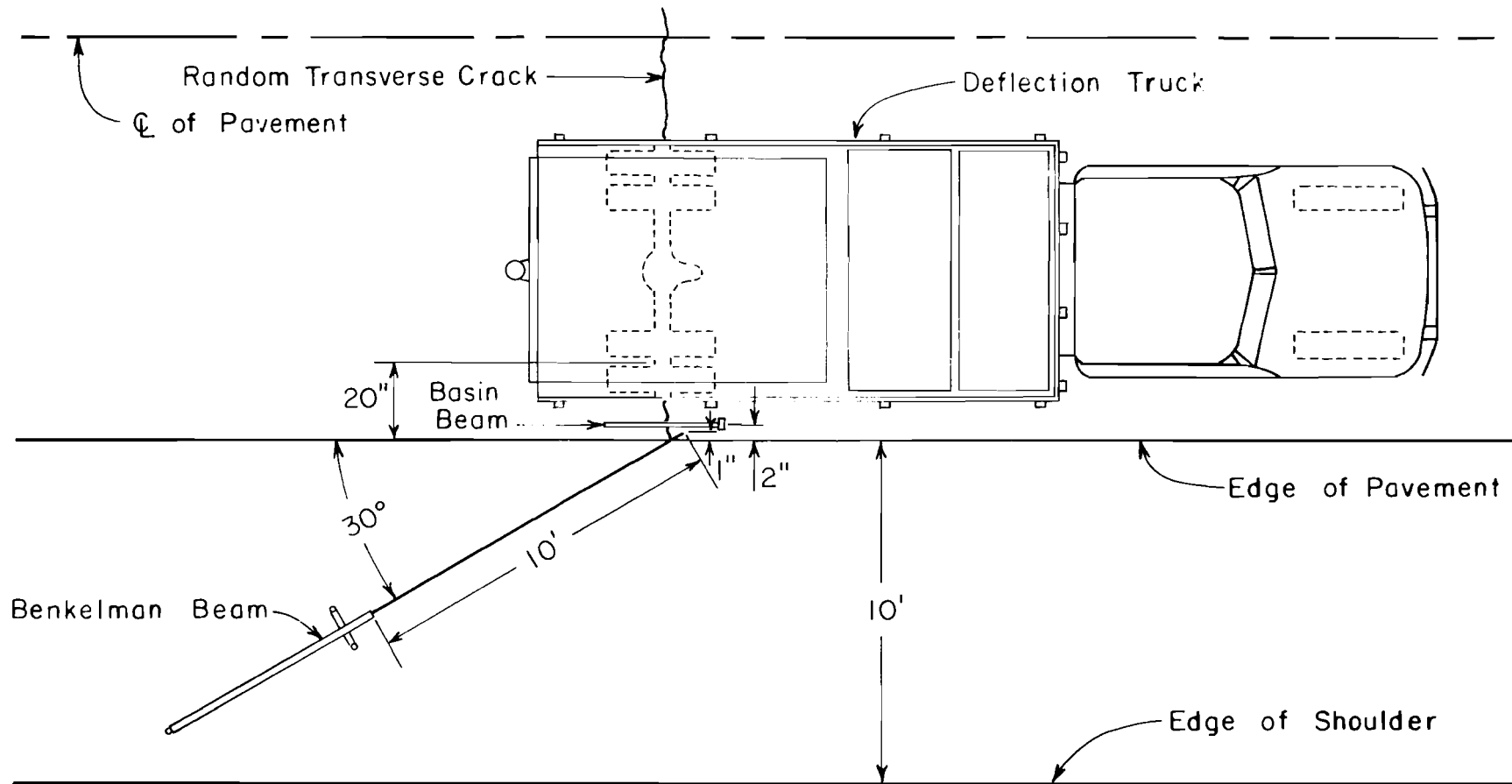
PLAN VIEW OF EQUIPMENT ARRANGEMENT

FIGURE A.1

Temperature Equipment. The special temperature
equipment used on this project was also designed by the
Research Section. It consisted of a small portable
eight-inch concrete slab in which two high speed resis-
tance thermometer bulbs were placed near the top and
bottom.[6] This equipment is shown in Figure A.2. The
leads from these bulbs were connected to a Minneapolis-
Honeywell Electronik Temperature Recorder which recorded
the top and bottom temperatures of the portable slab on
a continuous strip chart.

Microscope. A specially fabricated microscope with
a built-in scale in the eyepiece was used to measure the
width of the cracks. By setting the microscope over the
crack and focusing on it, the crack width could be read on
the inscribed scale to the nearest 0.002 inch. Figure
A.3 shows the microscope and Figure A.4 shows the built-in
scale.

Truck. The truck which was used to deflect the pave-
ments in this and continuing studies is a single axle
stake-type truck rated at three tons. It is equipped with
a box of lead shot for dead load and also a large water
tank so that the magnitude of the load can be varied.

The deflection truck was loaded such that the rear
axle load was 18,000 pounds and the tire inflation
pressure was 75 psi. The 18,000 pound single axle load
was adopted because it represents the maximum legal load
limit on a single axle in Texas, and it is used as the
basis for deriving equivalencies in the AASHO Design
method.[4]

Experimental Procedure

The procedures used at the AASHO Road Test were used
as guidelines in developing the procedure for this experi-
ment.[3] New procedures were required to study the CRCP
variables which are new to rigid pavement design.

At every 200 foot interval within the test section
and the replicate test section, measurements for radius of
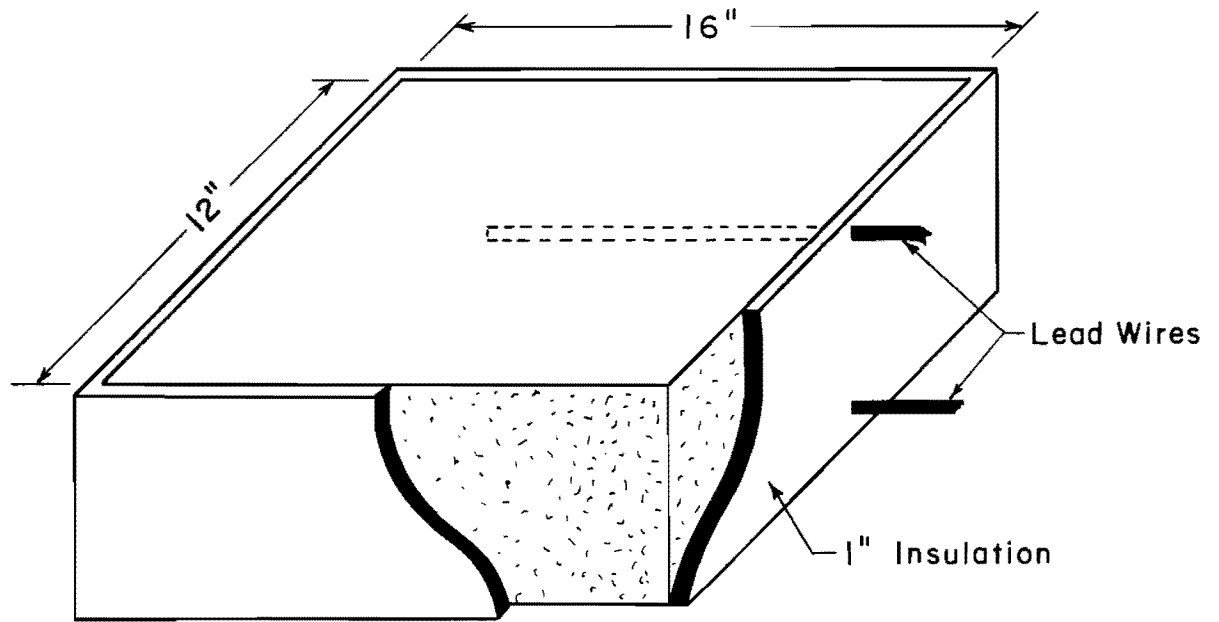
OVERALL VIEW
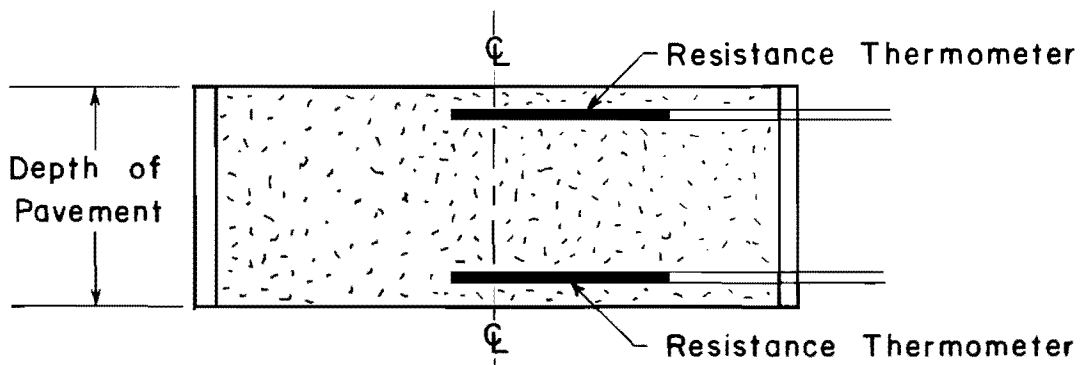
SECTION

TEMPERATURE SLAB

FIGURE A.2

Figure A.3.   Microscope Used
to Measure Crack Width
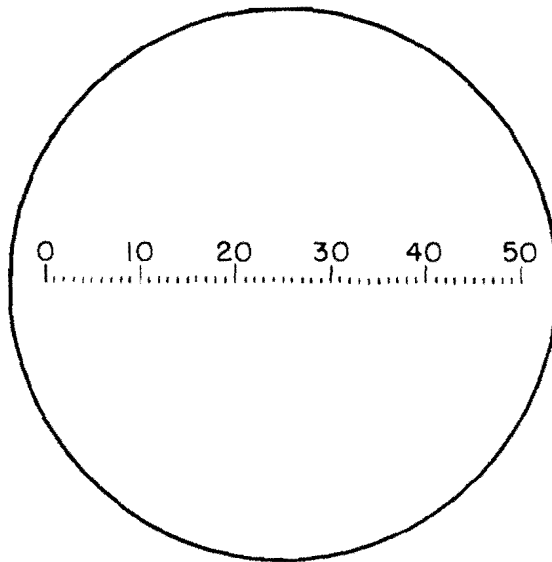
Figure A.4.   Graduated Eye-
piece of Microscope

APPENDIX   B

Deflection and Radius of Curvature Data Sheet

and

Summaries of Data

TEXAS HIGHWAY DEPARTMENT

	1		2	3		4		5	6	7		8
DEPTH		LINE			COLUMN		COUNTY				SECONDARY STUDY	

	9	10	11		12	13		14	15		16		17	18	19
CONTROL				SECTION			JOB			PART		$\bar{X}$			

	20		21		22	23	24	25		26	27	28	29
MOISTURE		TRAFFIC		BEGIN STAT.NO.					END STAT.NO.				

	30		31	32		33	34		35	36
BEAM NO		MONTH			DAY			YEAR		

TY D	D	TIME	T T	T B	Δ X	RADIUS OF CURV.	STAT. NO. AT DEFL.	DIST. FEET	"A" OUT	"B" OUT
37	38 39 40	41 42 43 44	45 46 47 48	49 50 51 52	53 54 55	56 57 58	59 60 61 62	63 64	65 66	67 68
								0		
								1		
								2		
								4		
								6		
								8		
								1 0		
								1 2		
								1 4		
								1 6		
								1 8		
								2 0		
								2 2		
								2 4		
								2 6		
								2 8		
								3 0		
								3 2		
								3 4		
								3 6		

COMMENTS:

TABLE B.I

TABLE B.2

DEFLECTION AND RADIUS OF CURVATURE DATA
- FALL -

(DEFLECTION IN THOUSANDTHS OF AN INCH AND CURVATURE IN FEET)

SUBGRADE SUPPORT	SUBBASE TYPE	SUBBASE MATERIAL	3,500,000 psi			5,500,000 psi		
			Low 580 psi	Medium 580-690 psi	High 690 psi	Low 580 psi	Medium 580-690 psi	High 690 psi
Poor 5.5 +	Non-Stabilized	Fine Grain		DC=17.2 RC=3979 DE=17.7 RE=12182			DC=10.7 DE=9.6	
		Crushed Stone		DC=15.1 RC=5834 DE=13.0 RE=11727			DC=22.5 DE=21.7	DC=7.9 RC=8620 DE=9.1 RE=19267
	Stabilized	Cement					DC=8.3 RC=13477 DE=6.6 RE=20132	DC=6.8 RC=11355 DE=3.7 RE=22249
		Asphalt						
		Lime	*DC=12.7 RC=11194 DE=8.8 RE=29444	DC=10.5 RC=9288 DE=10.6 RE=17266				
Fair 5.0 – 5.5	Non-Stabilized	Fine Grain		*DC=7.0 RC=7439 DE=10.5 RE=23241			DC=15.6 RC=3771 DE=9.3 RE=15314	
		Crushed Stone		DC=11.3 DE=10.2	*DC=6.6 DE=5.2			
	Stabilized	Cement					DC=6.7 RC=11416 DE=6.7 RE=19999	
		Asphalt		DC=10.1 DE=7.7				
		Lime		*DC=6.1 RC=10478 DE=5.6 RE=17578				
Good 4.0 – 5.0	Non-Stabilized	Fine Grain		DC=16.1 RC=3337 DE=9.8 RE=13355			DC=22.2 RC=4630 DE=20.6 RE=16924	
		Crushed Stone		DC=11.8 RC=9692 DE=10.7 RE=15291			DC=13.4 DE=13.3	DC=7.7 RC=7844 DE=11.0 RE=18806
	Stabilized	Cement					DC=5.3 RC=20752 DE=5.3 RE=33095	DC=5.1 RC=12243 DE=5.7 RE=26667
		Asphalt		DC=9.1 DE=9.2				
		Lime		DC=11.0 RC=4370 DE=11.7 RE=13525				

MODULUS OF ELASTICITY
CONCRETE FLEXURAL STRENGTH

* CURBED PAVEMENT SECTION

TABLE B.3

DEFLECTION AND RADIUS OF CURVATURE DATA
- WINTER -

(DEFLECTION IN THOUSANDTHS OF AN INCH AND CURVATURE IN FEET)

SUBGRADE SUPPORT	SUBBASE TYPE	SUBBASE MATERIAL	MODULUS OF ELASTICITY 3,500,000 psi			5,500,000 psi		
		CONCRETE FLEXURAL STRENGTH	Low 580 psi	Medium 580-690 psi	High 690 psi	Low 580 psi	Medium 580-690 psi	High 690 psi
Poor 5.5 +	Non-Stabilized	Fine Grain		DC=16.3 RC=5685 DE=17.1 RE=9451			DC=7.5 RC=6595 DE=7.7 RE=14360	
		Crushed Stone		DC=16.2 RC=5042 DE=14.4 RE=11672			DC=28.3 RC=5061 DE=31.0 RE=12375	DC=11.3 RC=6479 DE=8.7 RE=16663
	Stabilized	Cement		DC=8.4 RC=8955 DE=6.6 RE=29166			DC=10.9 RC=14067 DE=10.1 RE=26219	DC=7.4 RC=14761 DE=5.1 RE=23904
		Asphalt		DC=12.3 RC=7576 DE=8.7 RE=12601				
		Lime	*DC=1.8 RC=16229 DE=6.0 RE=23668	DC=5.2 RC=10375 DE=6.3 RE=19482				
Fair 5.0 – 5.5	Non-Stabilized	Fine Grain		*DC=4.9 RC=21826 DE=7.7 RE=26786			DC=14.5 RC=5831 DE=8.5 RE=13853	
		Crushed Stone		DC=12.1 RC=6254 DE=11.6 RE=13456	*DC=2.7 RC=38790 DE=3.3 RE=34921			
	Stabilized	Cement					DC=7.9 RC=12467 DE=9.4 RE=19451	
		Asphalt		DC=7.5 RC=8171 DE=7.9 RE=15224				
		Lime		*DC=6.3 RC=11310 DE=8.4 RE=19511				
Good 4.0 – 5.0	Non-Stabilized	Fine Grain		DC=14.0 RC=4437 DE=12.1 RE=12727			DC=10.6 RC=5466 DE=6.9 RE=15205	
		Crushed Stone		DC=12.1 RC=8970 DE=10.8 RE=17839			DC=12.9 RC=9575 DE 16.1 RE=14523	DC=14.8 RC=6847 DE=10.7 RE=16597
	Stabilized	Cement		DC=9.1 RC=6402 DE=6.8 RE=26389			DC=5.1 RC=13806 DE=4.5 RE=27118	DC=5.4 RC=16169 DE=3.8 RE=28600
		Asphalt		DC=8.7 RC=7212 DE=7.2 RE=14273				
		Lime		DC=7.7 RC=15856 DE=7.5 RE=19124				

* CURBED PAVEMENT SECTION

74

TABLE B.4
DEFLECTION AND RADIUS OF CURVATURE DATA
-SUMMER-

(DEFLECTION IN THOUSANDTHS OF AN INCH AND CURVATURE IN FEET)

Subgrade Support	Subbase Type	Subbase Material	3,500,000 psi Low 580 psi	3,500,000 psi Medium 580-690 psi	3,500,000 psi High 690 psi	5,500,000 psi Low 580 psi	5,500,000 psi Medium 580-690 psi	5,500,000 psi High 690 psi
Poor 5.5 +	Non-Stabilized	Fine Grain		DC = 17.6 RC=13624 DE =18.0 RE=14947			DC = 8.0 RC=14127 DE = 9.7 RE=15602	
		Crushed Stone		DC = 13.6 RC=11634 DE =12.5 RE=13119			DC = 19.8 RC=10517 DE =19.6 RE=11482	DC = 6.0 RC=16021 DE = 7.5 RE=19831
	Stabilized	Cement		DC = 6.9 RC=19957 DE = 4.9 RE=25377	DC = 15.0 RC=6786 DE = 13.5 RE=12750		DC = 8.6 RC=23659 DE = 6.3 RE=30556	DC = 3.3 RC=20332 DE = 3.8 RE=25321
		Asphalt		DC = 11.8 RC=10310 DE=12.2 RE=11248	DC=15.8 RC=5328 DE=10.8 RE=13826			
		Lime	*DC = 3.8 RC=25680 DE = 4.3 RE=21882	DC = 5.4 RC=20777 DE = 4.9 RE=23007				
Foir 5.0 – 5.5	Non-Stabilized	Fine Grain		*DC = 6.2 DE = 4.1			DC = 13.7 RC=10105 DE = 19.6 RE=10817	
		Crushed Stone		DC = 11.2 RC=9546 DE = 10.0 RE=12864	*DC = 2.7 RC=38790 DE = 3.3 RE=34921			
	Stabilized	Cement					DC = 7.6 RC=20014 DE = 6.2 RE=23265	
		Asphalt		DC = 7.5 RC=12450 DE = 9.0 RE=14607				
		Lime		*DC = 5.0 RC=25454 DE = 5.0 RE=27665				
Good 4.0 – 5.0	Non-Stabilized	Fine Groin		DC = 16.3 RC=9772 DE =16.9 RE=11262			DC=20.5 RC=10292 DE=20.0 RE=12347	
		Crushed Stone		DC= 10.5 RC=17923 DE =10.3 RE=21295			DC = 13.6 RC=15525 DE = 11.6 RE=14595	DC = 7.8 RC=18300 DE = 7.8 RE=21344
	Stabilized	Cement		DC = 5.3 RC=27249 DE = 5.0 RE=33333			DC = 4.7 RC=14274 DE = 4.3 RE=30045	DC = 5.3 RC=27052 DE 4.5 RE=39569
		Asphalt		DC = 6.8 RC=13481 DE = 9.4 RE=13538				
		Lime		DC = 9.1 RC=16033 DE = 8.0 RE=18526				

* CURBED PAVEMENT SECTION

TABLE B.5

DEFLECTION AND RADIUS OF CURVATURE DATA
-SPRING-

(DEFLECTION IN THOUSANDTHS OF AN INCH AND CURVATURE IN FEET)

SUBGRADE SUPPORT	SUBBASE TYPE	SUBBASE MATERIAL	3,500,000 psi			5,500,000 psi		
			Low 580 psi	Medium 580-690 psi	High 690 psi	Low 580 psi	Medium 580-690 psi	High 690 psi
Poor 5.5 +	Non-Stabilized	Fine Grain		DC=13.43 RC=14330 DE=11.77 RE=13853			DC=8.49 RC=9926 DE=8.43 RE=12556	
		Crushed Stone		DC=13.78 RC=10225 DE=14.34 RE=12666			DC=19.41 RC=12105 DE=19.08 RE=11593	DC=6.78 RC=9006 DE=6.93 RE=16120
	Stabilized	Cement		DC=6.46 RC=13321 DE=5.33 RE=22155	DC=11.37 RC=10235 DE=10.42 RE=15253		DC=4.25 RC=28139 DE=2.81 RE=31746	DC=7.12 RC=11119 DE=5.15 RE=25888
		Asphalt		DC=9.10 RC=6442 DE=7.46 RE=13264	DC=13.4 RC=12871 DE=17.02 RE=16497		DC=6.68 RC=14558 DE=5.92 RE=14815	
		Lime		DC=3.71 RC=13538 DE=2.96 RE=26871				
Fair 5.0 – 5.5	Non-Stabilized	Fine Grain		＊DC=4.90 RC=13859 DE=4.39 RE=30170			DC=8.04 RC=13719 DE=7.15 RE=15476	
		Crushed Stone		DC=8.58 RC=6825 DE=7.12 RE=14154				
	Stabilized	Cement					DC=6.48 RC=14487 DE=5.43 RE=19890	
		Asphalt		DC=6.87 RC=5813 DE=5.50 RE=13084			DC=6.32 RC=14324 DE=5.86 RE=15212	
		Lime		＊DC=5.21 RC=15659 DE=4.83 RE=20833				
Good 4.0 – 5.0	Non-Stabilized	Fine Grain		DC=10.02 RC=10981 DE=9.03 RE=15787			DC=9.17 RC=8858 DE=7.83 RE=14435	
		Crushed Stone		DC=6.38 RC=13774 DE=4.79 RE=31316			DC=7.26 RC=16034 DE=9.76 RE=18943	DC=6.20 DE=6.24 RE=14623
	Stabilized	Cement		DC=4.32 RC=15000 DE=4.33 RE=35374			DC=5.00 RC=17563 DE=3.41 RE=30584	DC=4.08 RC=24896 DE=3.69 RE=26496
		Asphalt		DC=8.68 RC=6318 DE=5.93 RE=13446				
		Lime		DC=11.04 RC=8480 DE=9.46 RE=16383			DC=4.17 RC=11463 DE=6.43 RE=18707	

MODULUS OF ELASTICITY
CONCRETE FLEXURAL STRENGTH

＊ CURBED PAVEMET SECTION

76

APPENDIX   C

Computer Print-Out of Typical Data

TEXAS HIGHWAY DEPARTMENT

DEPTH 8 LINE 1 COLUMN 5 COUNTY 236 SECONDARY STUDY 0 CONTROL 675 SEC 7 JOB 1 PART 3

AVERAGE CRACK SPACING 3.8 WET   TRAFFIC   BEGINNING STATION   0 ENDING STATION 25.00
BEAM NUMBER 4   MONTH 6 DAY 15 YEAR 1966

TYPE	DEFLECTION READING	CORRECTED	TIME	TEMPERATURE TOP	BOTTOM	DIFF	AVG	CRACK WIDTH SPACES	CONVERTED	CURVATURE READING	RADIUS COMPUTED	STATION	DIST	BASIN SEC A	BASIN SEC B
DC	.0052	.0101	0847	91.7	81.2	10.5	86.4	-0	0	.0013	12821	0		0	0
DC	.0052	.0101	0853	92.5	81.5	11.0	87.0	-0	0	.0013	12821	2.00		3	3
DC	.0049	.0094	0857	92.7	81.7	11.0	87.2	-0	0	.0015	11111	4.00		10	8
DC	.0039	.0074	0902	93.0	81.7	11.3	87.3	-0	0	.0015	11111	6.00		13	13
DC	.0032	.0060	0907	93.2	81.8	11.4	87.5	-0	0	.0012	13889	8.00		13	15
DC	.0028	.0051	0914	94.0	82.0	12.0	88.0	-0	0	.0012	13889	10.00		13	15
DC	.0025	.0045	0916	94.0	82.0	12.0	88.0	-0	0	.0014	11905	12.00		12	14
DC	.0032	.0060	0919	93.6	82.0	11.6	87.8	-0	0	.0014	11905	13.00		11	13
DC	.0030	.0055	0921	93.7	82.1	11.6	87.9	-0	0	.0016	10417	15.00		11	12
DC	.0050	.0096	0924	93.6	82.1	11.5	87.8	-0	0	.0016	10417	17.00		11	12
DC	.0039	.0074	0927	93.5	82.3	11.2	87.9	-0	0	.0011	15152	19.00		11	12
DC	.0030	.0055	0945	93.0	82.9	10.1	87.9	-0	0	.0011	15152	21.00		11	12
DC	.0029	.0053	0947	93.0	82.9	10.1	87.9	-0	0	.0010	16667	23.00		11	12
DC	.0035	.0066	0951	94.8	83.0	11.8	88.9	-0	0	.0010	16667	25.00		11	12

DEFLECTION	AVERAGE	DEVIATION	ERROR
A	.0075	.0022	.0008
B	.0066	.0014	.0005
AB	.0070	.0019	.0005

TEMPERATURE DIFFERENTIAL	AVERAGE	DEVIATION	ERROR
	11.3	.5	.2
	11.1	.7	.3
	11.2	.6	.2

CRACK WIDTH			
A	0	0	0
B	0	0	0
AB	0	0	0

MID-DEPTH TEMPERATURE			
	87.4	.5	.2
	88.0	.4	.1
	87.7	.6	.1

RADIUS OF CURVATURE			
A	12507	1087	411
B	13768	2579	975
AB	13137	2077	555

CORRECTED DEFLECTION
.00913
.00797
.00855

APPENDIX   D

Pavement Thickness - Deflection Analysis

PAVEMENT THICKNESS - DEFLECTION ANALYSIS

Figure D.1 is a graph of deflection on a six inch CRCP versus deflection on an eight inch CRCP, the lowermost line is that of the AASHO Road Test and the uppermost line is for the data taken on the CRCP.

For this analysis, the lines are all drawn through the origin. Therefore, the equation of the lines would be of the form $Y = MX$. From Phase I[2] studies in connection with this, the following expression was derived:

$$d = \frac{A_o L\ 10^{A_1 \Delta x}\ \bar{x}^{A_3}}{10^{A_2}\ T\ D^N}$$

Now let $\dfrac{A_o L\ 10^{A_1 \Delta x}\ \bar{x}^{A_3}}{10^{A_2 T}}$ equal a constant, K.

Therefore $\quad d_6 = \dfrac{K}{D_6^{\ N}}$ \hfill (5.2)

and $\quad d_8 = \dfrac{K}{D_8^{\ N}}$ \hfill (5.3)

Dividing Equation (5.2) by (5.3), assuming equal conditions except for thickness, the constant, K, drops out.

$$\frac{d_6}{d_8} = \frac{D_8^{\ N}}{D_6^{\ N}}$$ \hfill (5.4)

Using thickness of eight and six inches, the above reduces to the following equation:

$$\frac{d_6}{d_8} = \frac{8^N}{6^N} = 1.33^N$$ \hfill (5.5)

Using the previous assumption of passing all lines through the origin the slope of any line on Figure D.1 would be:

$$\text{Slope of line} = \frac{d_6}{d_8} = M \qquad (5.6)$$

Equating equations (5.5) and (5.6):

$$M = 1.33^N$$

$$\log M = N \log 1.33$$

$$N = \frac{\log M}{\log 1.33} = \frac{\log M}{0.124}$$

From AASHO Road Test studies:

$$N = 1.178$$

$$1.178 = \frac{\log M}{0.124}$$

$$\log M = 0.146$$

$$M = 1.40 \text{ (slope of solid line, labeled AASHO)}$$

The dashed line is the result of work in Texas on CRCP. For the Texas study M = 1.65, thus can calculate N value.

$$N = \frac{\log M}{0.124} = \frac{\log 1.65}{0.124}$$

$$N = 1.75$$

The line labeled Westergaard on Figure D.1 represents the relationship predicted by Dr. H. M. Westergaard in his theory.[16] In Westergaard's equation the pavement thickness has an exponent of 1.5. Thus the result of the study on continuously reinforced concrete pavement compares quite well with theoretical predictions.
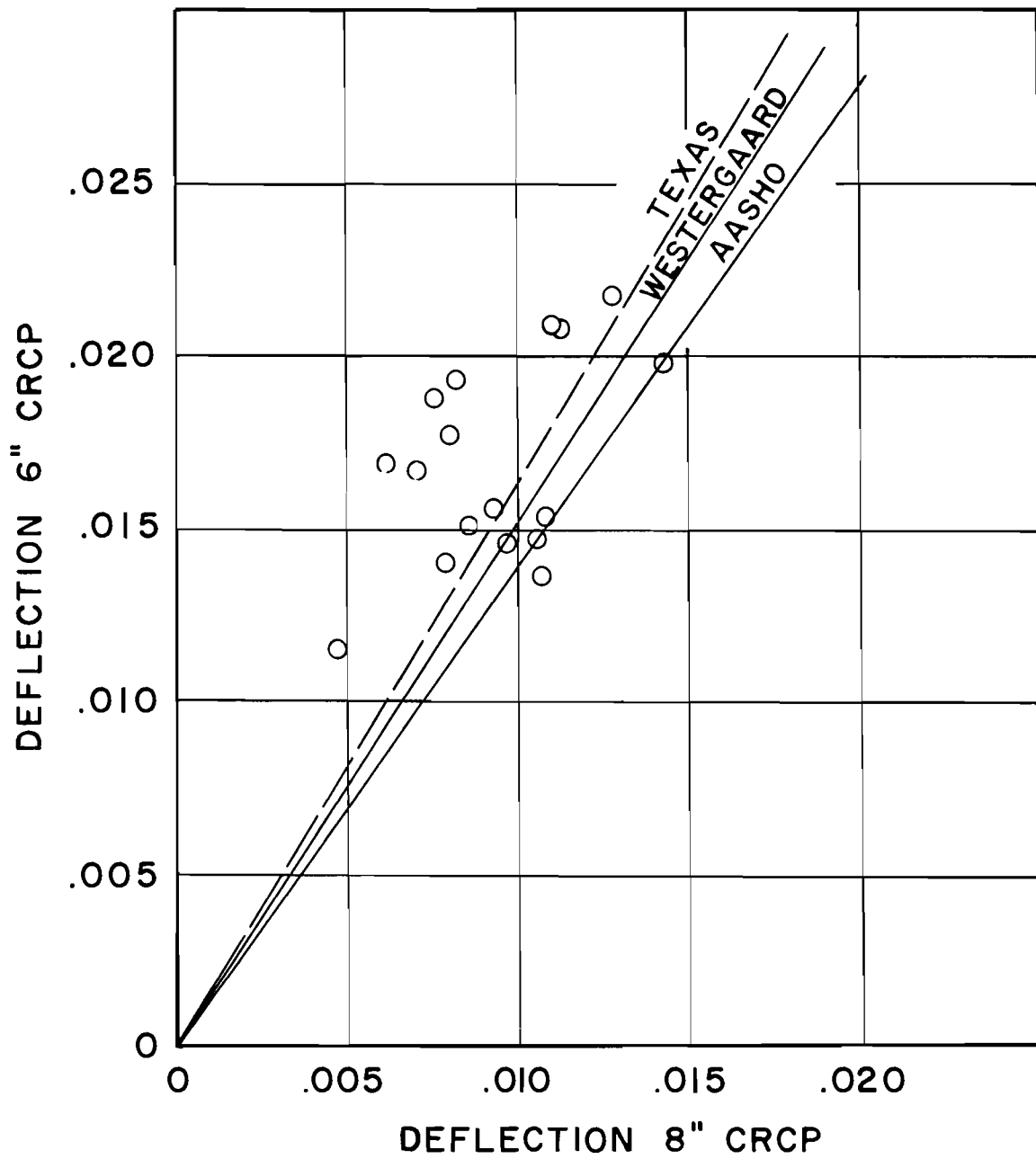
DEFLECTION ON SIX AND EIGHT
INCH THICK CRCP

FIGURE D.1

APPENDIX   E

Deflection of CRCP on a Wet Foundation

DEFLECTION OF CRCP ON A WET FOUNDATION

As mentioned earlier in this report, the last of the
four data runs was made in the spring of 1965 which was
an extremely wet season in the eastern half of the State
of Texas. All of the deflections measured on this
fourth run were significantly smaller than deflections
measured previously on the same test sections:

A special deflection run was made on 18 test sections
in the late spring and early summer of 1966 when the pave-
ment foundation was wet to spot check the fourth run data.
The results revealed almost identical trends as the fourth
run in 1965.

The data was compared to and plotted against the 1965
data on the same test sections. Identical data would fall
on a 45 degree line. The graph of this data is shown
in Figure E.1. The closeness of the data is revealed by
the graph. Note that most of the data is very near the
45 degree line. This special run thus validates the
fourth run data and indicates that CRCP on a wet foundation
deflects less than one on a dry foundation.
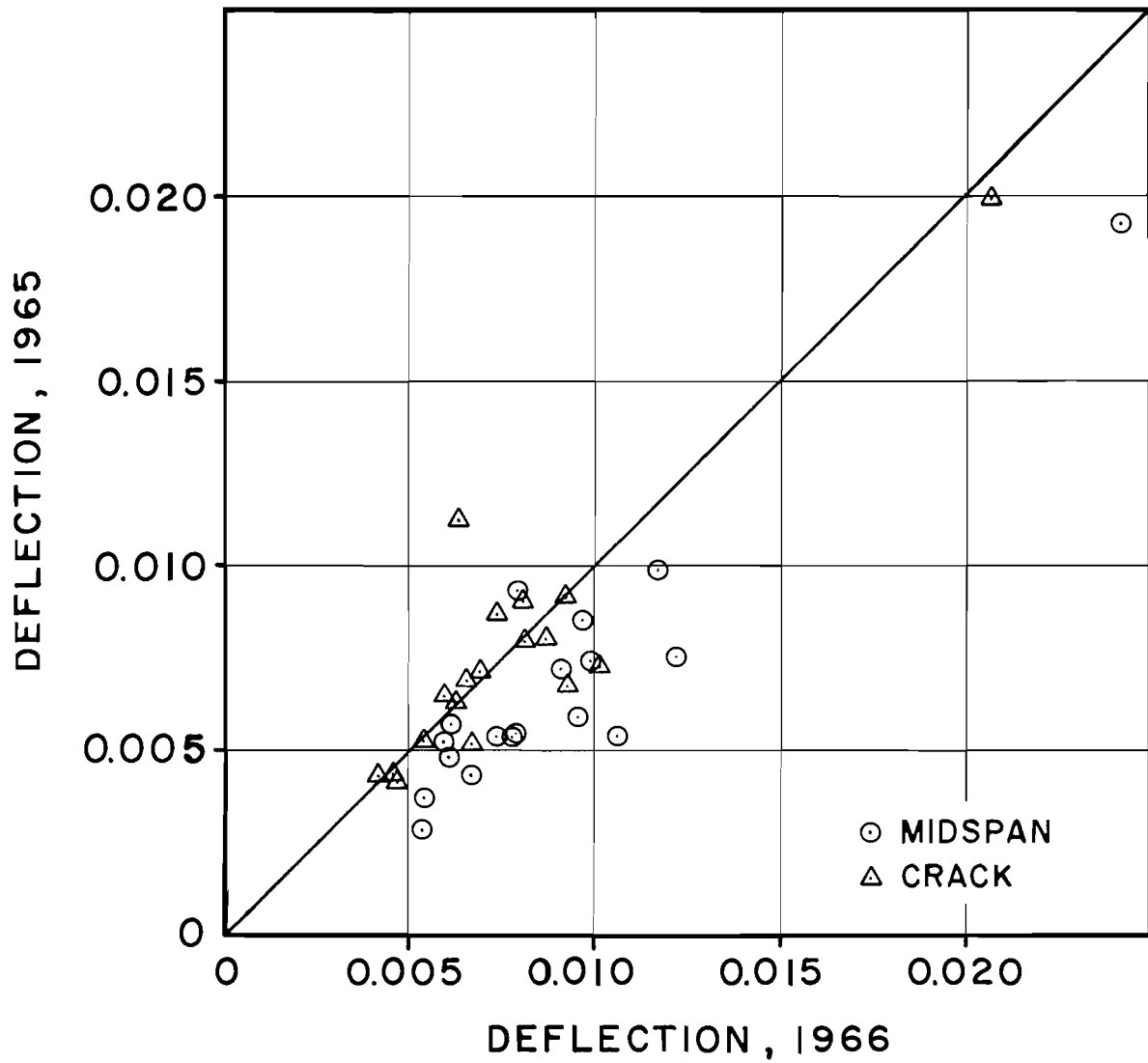
CRCP DEFLECTION ON WET FOUNDATION
1965 & 1966

FIGURE E.I

APPENDIX F

Notes of Soil Support

NOTES OF SOIL SUPPORT

When the test sections were initially classified in the factorial, lime stabilization of the subgrade was not accounted for. Early analysis revealed that the test sections with lime treated subgrades showed better performance than was expected for that particular factorial entry.

When the soil support values were calculated for each test section the lime treated subgrades were accounted for. The soil support values were calculated from the equation,

$$SS = \left(\frac{U_1 + U_2}{T_{sg}}\right)^{1/4}$$

Where:

U = Unconfined compressive strength of the subbase at the age of seven days

T = Texas Triaxial Classification of the subgrade

1, 2 = subscripts denoting subbase and stabilized subgrade, respectively.

Experience indicates that the lime treated subgrade acted as a second subbase. Using this observation as support, the seven day strength of the lime treated subgrade material was added to that of the subbase. It was impossible to obtain the subgrade strengths for the test sections, and therefore, a value of 200 psi was assigned to each subgrade strength. This helped to correlate both deflection and radius of curvature to the soil support.